20 WINTHROP SQUARE, 2ND FLOOR, BOSTON, MA 02110 617.728.7000

GEN3 PARTNERS

Validation of the Observation of Soft X-ray Continuum Radiation from Low-Energy Pinch Discharges in the Presence of Molecular Hydrogen

Alexander Bykanov, PhD

Spectroscopy was performed at the Harvard Smithsonian Center for Astrophysics (CfA), Cambridge, MA, USA by CfA spectroscopists under contract to GEN3 Partners

Abstract

Spectra of low-energy high current pinch discharges in pure molecular hydrogen and helium were recorded in the EUV region at the Harvard Smithsonian Center for Astrophysics, Cambridge, MA, USA (CfA) in an attempt to reproduce experimental results published by BlackLight Power, Inc. showing continuum radiation only from hydrogen [1-2]. Alternative explanations to the claimed explanation of the observation of predicted continuum radiation at 10.1 and 22.8 nm and going to longer wavelengths for transitions of H to lower-energy states were considered. The continuum radiation was observed at CfA in the 10–30 nm region that comprised two bands with one having a short wavelength cutoff at about 10 nm and another was identifiable as a slope change on the first at about 23 nm. Considering the low energy of 5.2 J per pulse, the observed radiation in the energy range of about 120 eV to 40 eV, and reference experiments with He, no conventional explanation was found to be plausible including electrode metal emission, Bremsstrahlung radiation, ion recombination, molecular or molecular ion band radiation, and instrument artifacts involving radicals and energetic ions reacting at the CCD and H_2 re-radiation at the detector chamber.

I. Introduction

BlackLight Power, Inc. (BLP) reported the observation of continuum radiation from high-current gas discharge in the presence of molecular H_2 in the discharge chamber [1-2]. Spectra were measured with a vacuum grazing incidence spectrometer and recorded with a back-illuminated CCD camera. The gas pressure was varied in the range from 0.1 to 1.3 Torr. The spectrometer calibrated with O (and He) lines showed reliable wavelength measurements. Mills predicted that atomic hydrogen forms fractional

GEN3 PARTNERS

Rydberg energy states $H(1/p)$ called "hydrino atoms" wherein $n=\frac{1}{2},\frac{1}{3},\frac{1}{4},...,\frac{1}{p}$ ($p \le 137$ is an integer) replaces the well-known parameter $n=\text{integer}$ in the Rydberg equation for hydrogen excited states [1-4]. The transition of H to $H\left[\frac{a_H}{p=m+1}\right]$ occurs by a nonradiative resonance energy transfer of $m \cdot 27.2\ eV$ to m H atoms (m is an integer) to form an intermediate that decays with the emission of continuum bands with short wavelength cutoff and energies $E_{\left(H\to H\left[\frac{a_H}{p=m+1}\right]\right)}$ given by

$$E_{\left(H\to H\left[\frac{a_H}{p=m+1}\right]\right)}=m^2\cdot 13.6\ eV\ ;\ \lambda_{\left(H\to H\left[\frac{a_H}{p=m+1}\right]\right)}=\frac{91.2}{m^2}\ nm \quad (1)$$

and extending to longer wavelengths than the corresponding cutoff. This theory explains the photon energy range observed in the plasma emission experiments with molecular hydrogen. BLP funded a study conducted by GEN3 Partners, Boston, MA to substantiate or demolish these findings involving reproducing the spectral measurements at the CfA and the evaluation of possible alternative explanations by plasma physicist A. Bykanov.

II. Experimental Method

The BLP light source loaned to CfA and the experimental set up for recording the EUV spectra of pulsed plasmas using molybdenum (Mo), tantalum (Ta), and tungsten (W) electrodes are shown in Figures 1 and 2. These electrodes and test equipment including the high-voltage supplies, turbo pumps, back-illuminated CCD and CCD data processing equipment were also provided by BLP. Spectra of EUV radiation emitted from pure helium and pure hydrogen plasmas were recorded at CfA using CfA supplied UHP helium and hydrogen gas supplies. Additional spectra were recorded for helium-hydrogen mixtures at BLP. The spectra were recorded at CfA using a BLP-loaned McPherson grazing incidence EUV spectrometer (Model 248/310G) equipped with a platinum-coated 600 g/mm or a platinum-coated 1200 g/mm grating. The angle of incidence was 87°. The wavelength resolution was about $0.05\ nm$ with an entrance slit width of <1 μm. The EUV light was detected by a CCD detector (Andor iDus) cooled to –60 °C. In addition, CfA provided a McPherson 310g spectrometer with a platinum-coated 1200 g/mm and a 133 g/mm grating. Both spectrometers and all CfA and BLP gratings were used as part of the measurement program as indicated in captions for Figures 3A-D and 4A-J.

The main BLP discharge cell comprised a hollow anode (3 mm bore) and a hollow cathode (3 mm bore) with electrodes made of Mo, Ta, or W (see Figure 1). The electrodes were separated by a 3 mm gap. A high voltage DC power supply was used to charge a bank of ten pairs 5200 pF capacitors connected in parallel to the electrodes. The cathode was maintained at a voltage of –10 kV before the triggering, while the anode was grounded. In some experiments, the voltage was increased up to -15 kV to determine the

influence of this parameter on the observed spectra. An electron gun (Clinton Displays, Part # 2-001), driven by a high voltage pulse generator (DEI, PVX 4140), provided a pulsed electron beam with electron energy of 1-3 kV and pulse duration of 0.5 ms. The electron beam triggered a high voltage pulsed discharge at a repetition rate of 5 Hz.

Radiation was measured through aperture limiting gas flow from the discharge chamber into the detector chamber. Two-stage differential pumping resulted in low gas pressure in the detector chamber (in the range of 1E-6 Torr) while the gas pressure in the discharge chamber was maintained in the range from 0.1 to 1.3 Torr.

In all cases (BLP and CfA experiments), the BLP discharge cell was aligned with the spectrometer using a laser. The CCD detector was gated synchronously with the e-beam trigger. It had an exposure time of 100 ms for each discharge pulse having a breakdown time of about 300 ns. Each recorded spectrum accumulated radiation from 500 or 1000 discharges and in one case 5000 discharges. The CCD dark count was subtracted from the accumulated spectrum. The wavelength calibration was confirmed by OV and OVI lines from the oxygen present on the electrodes in the form of metal oxides. Typical flow rates of ultrahigh purity helium, hydrogen, and mixtures (at BLP), deuterium (at BLP), oxygen (at BLP), and oxygen-hydrogen mixtures (at BLP) ranged from 1 to 10 sccm, and the pressures in the discharge chamber were maintained between 100 mTorr and 1300 mTorr controlled by a mass flow controller (MKS). Both on-line mass spectroscopy and high-resolution visible spectroscopy using Jobin Yvon Horiba 1250 M spectrometer [1-2] were used for monitoring contaminants in the plasma forming gases (BLP).

Additional experiments were conducted at BLP to test issues regarding conventional explanations of the radiation (Section III). Plasmas in pure oxygen (90 mTorr) and oxygen-hydrogen mixtures (total pressure ~300 mTorr) were measured for testing oxygen emission due to the oxide coating on the electrodes and for hydroxyl radicals, respectively. Using a common set of W-electrodes, the EUV spectra of helium-hydrogen (100% to 17%) mixtures were recorded to demonstrate the emission on a common intensity scale. Hydrogen at increasing pressure over the range of 2.2 mTorr to 16 mTorr was flowed into the EUV detector chamber while the EUV spectra of pure helium and pure hydrogen were recorded to verify possible artifacts involving H_2 re-radiation and H-radicals recombination on the detector surface. The pure helium and pure hydrogen EUV spectra were recorded using an Al (150 nm thickness, Luxel Corporation) or a polyimide filter (110 nm thickness, Luxel Corporation) to demonstrate that the soft X-ray are emitted from the plasma and exclude a possible instrumental artifact involving radicals or energetic ions reacting at the CCD. The hydrogen gas pressure in the CCD detector chamber was monitored using a Varian Thermocouple pressure gauge. The CCD detector position in the beam

dispersed by the grating was changed from being centered at 20 nm to 10 nm to determine the short-wavelength cutoff of the hydrogen continuum radiation using the 600 g/mm grating and Ta electrodes.

III. Basic Experimental Results

Spectra of discharges in high purity helium were measured as reference for validation of the continuum-free spectra in absence of hydrogen in a manner similar to that of BLP [1-2]. The EUV spectra of electron-beam-initiated, high-voltage pulsed gas discharges in helium using different electrodes, gratings, spectrometers, and numbers of CCD image superpositions are shown in Figures 3A-D and the dashed traces of Figures 4A-C, E, I, and J. The known helium ion lines were observed in the absence of any continuum radiation. Oxygen ion lines were also observed similarly in all spectra including those from hydrogen discharges shown in Figures 4A-J due to the oxide layer on the metal electrodes.

In contrast, the continuum band was observed when pure hydrogen replaced helium. The emission spectra of electron-beam-initiated, high-voltage pulsed discharges in pure hydrogen recorded by the EUV grazing incidence spectrometer with Mo, Ta, and W electrodes and different gratings, spectrometers, and numbers of CCD image superpositions are shown in Figures 4A-J. Continuum radiation was observed from hydrogen discharge regardless of the electrode material, spectrometer or grating. However, the intensity of the emission from Mo electrodes was weaker than that of Ta and W at the short wavelengths. The vapor pressure of Mo at T=2400K is 0.0189 Pa; whereas, the vapor pressure of W and Ta are 1.59 X 10^{-6} Pa and 5.21 X 10^{-7} Pa, respectively, at this temperature [5]. The high metal vapor pressure of Mo during the pulse is expected to cause the plasma to be optically thick. This is supported by the absence of strong ion emission at the short wavelengths (<22 nm). As shown in Figure 4, the continuum width and features of the spectra obtained using Ta and W electrodes can be achieved by increasing the intensity using a more efficient grating and by increasing the number of superpositions. The continuum is not attributed to oxygen ions or hydroxyl radicals as shown in Figures 5A and 5B, respectively. No continuum was observed from pure oxygen discharge; but the continuum appeared in mixtures of O_2 and H_2 having an intensity proportional to the hydrogen partial pressure. This dependency of the continuum intensity on the H_2 pressure was also observed in helium-hydrogen mixtures. As shown in Figure 6, the continuum intensity increased with hydrogen concentration in helium-hydrogen mixtures, and the spectrum approached that of pure hydrogen at high H_2 concentration further eliminating electrode metal lines as the source of the continuum.

Considering the common features and the source of increased emission intensity involving different electrodes, gratings, spectrometers, and numbers of CCD image superpositions, the continuum profile was assigned by the CfA group to the same emitter with a variation in the observed extent in the region 10 nm to 30 nm depending on the sensitivity of the detection and optical thickness of the plasma.

Figures 4A-J and Figure 7 show that the hydrogen continuum radiation comprises two profiles, one with a short wavelength cutoff at about 10 nm and a second is distinguishable by a reversal of the slope of the intensity versus wavelength in the region of 22-23 nm. Conventional mechanisms of the continuum radiation unique to hydrogen in a region wherein hydrogen was previously not known to emit were sought.

Summarizing the basic spectral measurements, we may formulate the following:

1. The CCD camera records some signal attributed to a continuum spectrum ranging from 12 to 30 nm only in presence of H_2. No continuum was observed for neat He gas.
2. The intensity of the continuum spectrum scales proportionally to H_2 concentration in the mixture with He or O_2.
3. The width of the band depends on grating and electrode material. Typically the continuum radiation is observed as bell-shape band with peak located approximately between the edges. Table 1 shows the observation of the bands in nm and corresponding photon energies in eV.

Table 1. Observed Edges of the Continuum band.

Grating	**Electrode Material**		
	Mo	W	Ta
600 lines/mm	-	12 nm-30 nm (103 eV-41 eV)	15 nm-30 nm (83 eV-41 eV) 13 nm-30 nm (95 eV-41 eV)
1200 lines/mm	22 nm-28 nm (56 eV-44 eV)	15 nm-28 nm (83 eV-44 eV) 17 nm-28 nm (73 eV-44 eV)	17 nm-28 nm (73 eV-44 eV)

4. Spectra taken with an Al filter each exhibit a sharp edge on the continuum band corresponding to the transmission edge of the filter.

IV. Analysis and Supporting Experimental Results

A. Estimates for the Plasma Parameters

Before starting the search for an explanation of the observed spectra, we need to understand the range of plasma parameters, especially the plasma temperature. We will use scaling relations for a similar type of discharge having a known temperature. The discharge geometry run by BLP and repeated at the

GEN3 PARTNERS

CfA (Figures 1 and 2) is related to a Z-pinch type discharge. The pinch effect arises from the compression of the plasma by the magnetic field of the plasma current as first described in 1934 by W. H. Bennett [6]. In the classical Z pinch, the current flows along the z-axis of a cylindrical plasma volume. The lines of force of the magnetic field B created by the current comprise concentric circles arranged in planes perpendicular to the z-axis. Specifically, the resulting electrodynamic force F acting on a unit gas volume with a current density j is equal to $c^{-1}\mathbf{j}\cdot\mathbf{B}$, where c is the light velocity. F is directed inward along the radius of the cylindrical axis and causes the compression of the current channel. The gas-kinetic pressure of the plasma opposes the magnetic compression. At equilibrium the moving boundary of the pinch is a surface of equal pressure. From this condition, the so-called *Bennett equilibrium* follows:

$$\frac{B^2}{8\pi} = 2nkT \tag{2}$$

where T is the plasma temperature and n is the gas number density. This equation defines the magnetic pressure created by the plasma current. Further considerations suggest more adequate and correct models for plasma dynamics, but the simple Eq. (2) roughly gives the relation between current (proportional to B), plasma number density, and temperature:

$$nT \propto B^2 \propto I^2 \tag{3}$$

Now we can scale the temperature with the discharge current according to the known relationship:

$$T \propto I^k \tag{4}$$

wherein k may vary from 0.5 to 1 corresponding to the strong dependence of the plasma temperature on current (k>=0.5) that is in turn limited by the current power law due to the limiting number density increase (k<=1). Discharges of this type correspond with high accuracy to equilibrium discharges having an equilibrium between the electron temperature T_e and the ion temperature T_i [7]. Known plasma parameters of Z-pinch discharges are similar to another type of pinch discharge, the dense plasma focus (DPF) discharge that was extensively studied for EUV lithography. In a DPF discharge of Mather or, similar, Filippov geometry (Figure 8) the anode and cathode are coaxial electrodes [7]. For EUV sources, the discharge is created in a mixture of Xe and He at a total pressure <1 Torr, similar to the conditions of the BLP source. The spectra measured for these discharges are in the same band (from 5 to 20-30 nm). Unfortunately, there are no publications on measurement of spectra from H_2.

Typical parameters of the DPF pulse are as follows:

Output Capacitor	1.33 μ F
Voltage	4.5 kV
Energy	$CU^2/2$ ~13.5 J
Discharge rise time	~150 ns

GEN3 PARTNERS

Peak current	2CU/t = 80 kA

The measured spectra and EUV energy show that temperature was optimized for the generation of 13.5 nm radiation corresponding to the plasma temperature of 20-30 eV [7].

The parameters of the BLP pulsed power supply are as follows:

Capacitor	104 nF
Voltage	10 kV
Energy	5.2 J
Discharge time	300 ns (defined by the capacitance and inductance)
Peak current	7.0 kA

One can see that the BLP discharge is much less energetic than the DPF optimized for 13.5 nm radiation. If we use the scaling relation given by Eq. (4) for the temperature, we get a BLP-device plasma temperature ranging from 2 up to 9 eV. In any case, we cannot expect the temperature of the discharge to be higher than 15 eV.

B. Conventional Classical Mechanisms of Continuum Spectral Radiation

Classical theory suggests three mechanisms of continuum radiation from plasmas [8, 9]:

1. Bremsstrahlung radiation
2. Recombination radiation
3. Band radiation for molecular electronic transitions broadened by vibrational and rotational transitions

The first two can be excluded because the intensity of the emission caused by both ion recombination and Bremsstrahlung radiation decreases exponentially to shorter wavelengths; whereas, we observe a bell-shaped continuum band. It is possible that this shape may be the convolution of the spectra with the instrumental function of the spectrometer, but this instrument artifact is eliminated by control spectra and the effect of filters as presented in Sections IVC-E. In addition to the mismatch of the expected radiation profiles to that observed, these mechanisms can be excluded based on the spectral intensity dependence on the ion charge [9]. The relationships for Bremsstrahlung and recombination radiation are given by:

$$\frac{dE_{eff}}{d\nu} \sim \sum_i n_e n_i Z_i^2 \frac{\exp(-h\nu / kT)}{(kT)^{1/2}} \tag{5}$$

and

$$\frac{dE_{eff}}{d\nu} \sim n_e n_{i+1} Z_i^4 \frac{\exp(-(h\nu - \chi_{i,n})/kT)}{(kT)^{3/2}} \quad (6)$$

respectively. One can see from Eqs. (5-6) that in the former case, the intensity scales as Z squared and in the latter case, it scales as Z to the fourth power. Helium may have Z=2, but H_2 or H is restricted to only Z=1, which means that we should have observed continuum radiation associated with these mechanisms in helium rather than in H_2, the opposite of the results.

The influence of electrons triggering the discharge (electron gun) was also eliminated as the source of the continuum radiation. The applied pulsed voltage to drive the plasma was increased from -10 kV to -15 kV in sequential runs to determine any high-energy electron effect on the spectral profile. No effect was observed; thus, high-energy electrons were eliminated as a possible cause of continuum radiation.

C. Analysis of H_2^+ Radiation as the Source

Figure 9 shows molecular terms of the H_2 molecule [10]. One can see that all excited states of neutral H_2 are below 20 eV. Thus, neutral H_2 radiation cannot explain the soft X-ray radiation having photon energies exceeding 40 eV. On the other hand, the ground state of H_2^+ ion has ground level above 15 eV. But, H_2^+ has no excited state spectrum [11-13], and the second ionization energy of the hydrogen molecule, IP_2, of 16.2494 eV is given by the sum of the ionization energy of the hydrogen atom (13.59844 eV) [14] and the bond energy of H_2^+ (2.651 eV) [15] according to the levels shown in shown in Figure 9. Thus, H_2^+ emission >40 eV and as high as 125 eV is not possible.

There are several other objections for assigning the source of the high-energy continuum radiation to H_2^+ emission. The first objection regards the fairly large width of the observed band. The continuum ranges from ~40 to >100 eV covering the band of at least ~60 eV; although, the plasma temperature from our estimates does not exceed 15 eV and is likely less than ~9 eV. Vibrational-rotational broadening of electronic transition cannot be so broad (60 eV) in a plasma with a temperature of 10-15 eV, the vibrational-rotational levels cannot be populated even if they exist.

Deuterium was substituted for hydrogen, and the continuum was indiscernibly changed. At the resolution of 0.05 nm, predicted differences on the order of 0.15 nm at the longer wavelengths should have been observed. With sufficiently high resolution, EUV spectroscopy is capable of absolutely testing for the absence of the required isotope shifts of the molecular emission corresponding to a vibrational energy difference of up to 40%. Then, BLP's explanation of atomic radiation would be further confirmed [1-2]. The molecular band emission as the continuum source is already eliminated by the extraordinary energy mismatch argument.

GEN3 PARTNERS

D. Possible Artifact: Re-radiation of H_2 Inside of the Spectrometer

Next, several possible artifacts which may result in the observation of the continuum spectrum are considered. At least two of these artifacts are based on presence of H_2 in the spectrometer chamber. First, consider that the artifact may be the absorption of radiation from the plasma by H_2 in the spectrometer chamber that is re-radiated (at longer wavelength) from the bulk without any wavelength selection. This radiation will be imposed on the actual spectrum. The intensity profile observed on CCD may be explained by existence of the light path connecting the CCD to the chamber (Figure 1) and any minor gas passage around the slit mechanism. Figure 10 shows the absorption cross-section for H_2 and He from the database of LBL (Blue and Magenta respectively) as well as experimental data [16-18]. One can see that absorption cross section is fairly high for making a noticeable contribution to the CCD image. For comparison, He has a higher cross-section than H_2 by a factor of 2-3, but He has a long wavelength cut off edge at ~50 nm. Most of the radiation from plasma may be in EUV range above 50 nm where H_2 is a more efficient re-radiator than helium.

This possible artifact was directly eliminated by the results of subsequent experiments suggested to BLP. Specifically, hydrogen was flowed into the CCD detector chamber during pulsed discharges in pure helium and pure hydrogen wherein the pressure in the detector chamber was varied in the range from 2.2 mTorr to 16 mTorr. The EUV spectra were recorded, to test the mechanism that the observed continuum profile was due to instrument artifacts involving H_2 re-radiation at the detector. The hydrogen gas pressure was monitored using a Varian Thermocouple pressure gauge. As shown in Figure 11A, the helium spectrum of ion lines was unchanged with an attempt to create the artifact by flowing 1.2 mTorr of hydrogen into the CCD detector chamber. No continuum was observed from He plasma with H_2 added into the CCD detector chamber. Furthermore, the hydrogen continuum intensity shown in Figures 11B-C was not affected by the presence of hydrogen in the chamber at any pressure over the range. The possibility of an instrument artifact involving H_2 re-radiation at the detector was further eliminated by showing that the continuum radiation source was the plasma and that the CCD output was a real spectrum. Both aspects were shown using filters that predictably chopped the continuum spectrum and via the spectral shape change with the position of the CCD focus as discussed in Sections IVE and IVF.

E. Possible Artifact: Recombination of H Radicals on the CCD Surface

The Andor iDus CCD detector utilized in the verification of BLP's continuum radiation experiments is temperature sensitive. The DUV and EUV radiation coming to the spectrometer chamber may be absorbed by H_2 molecules (see absorption cross-section in Figure 10) and result in their dissociation. In the interest of not excluding any possible mechanism, we must also consider H radical formation in the discharge chamber and buffer chamber that penetrate into the spectrometer chamber through the connecting light path. Then, hydrogen radicals will recombine on the wall wherein a third

body is required for energy release and three-body collisions are not otherwise possible under these conditions. When H radicals recombine on the CCD surface releasing 4.5 eV/molecule, an increased dark current may be observed for certain zones of the CCD array resulting in the possibility of an artifact observed as a continuum spectrum. The bell-shaped profile may be formed by the profile of the H radicals in the light-path connection (pipe) from the spectrometer chamber to the CCD. A second explanation of the observed profile is EUV-radiation induced recombination (or migration) of H radicals over the CCD surface. This is a rather hypothetical mechanism that needs additional study. The artifact produced by radicals recombining on the CCD surface explains the variation of the observed spectra of Mo electrodes having less intensity in the short wavelengths than Ta and W based on different recombination rates of the radicals and subsequent drift of these radicals along the CCD surface.

The experiments, described in the previous section prove that the observed continuum radiation is not influenced by the hydrogen pressure in the detector chamber. This result proves that the corresponding artifact may be excluded.

Additional experiments were performed by BLP that directly prove the true nature of the continuum spectra and exclude artifacts related to H radicals. Pure helium and pure hydrogen EUV spectra were recorded using an Al (150 nm thickness, Luxel Corporation) or polyimide filter (110 nm thickness, Luxel Corporation) having the transmission curves shown in Figures 12 and 13, respectively, to demonstrate that the soft X-ray emission was from the plasma gas and not an instrument artifact involving radicals and energetic ions (Section IIIF) reacting on the CCD. The filter was placed in between the grating and the detector as shown in Figure 1. The intensities of the oxygen ion spectrum from the helium discharge (Figure 14A) and the continuum spectrum from the hydrogen discharge (Figures 14B-C) were all blocked on the short-wavelength side by the application of an Al filter in a manner that matched the filter transmission characteristic (Figure 12). The intensities of the helium ion spectrum from the helium discharge (Figure 15A) and the continuum spectrum from the hydrogen discharge (Figure 15B) were both blocked on the long-wavelength side by the application of a polyimide filter in a manner that matched the filter transmission characteristic (Figure 13).

In summary, radiation-induced recombination cannot explain the sharp edge observed with an Al filter if observed since the corresponding recorded spectrum has no relationship to the light dispersion from the grating. The same applies on the long-wavelength side for the application of a polyimide filter. Thus, cutoff filters to the short and long wavelengths sides of the continuum radiation were applied to prove that the source of the radiation was the plasma and that there is a dependency of the spectrum on the grating dispersion of the emission. The observed filter results confirm that the continuum emission originates from the discharge cell and not from the CCD detector and that the CCD output is a true spectrum.

F. Possible Artifact: H ions Generated by the Pinch

A similar possible artifact to that caused by radicals reacting at the CCD is that produced by energetic ions. A pinch discharge may generate energetic ions with energies up to several kV [7]. Hydrogen ions with such energies may bounce from the diffraction grating and hit the CCD surface, but it could be argued that helium would cause same effect, except that velocity would be one half that of H. In addition, ions could not pass either the Al or polyimide filter; yet, the spectrum is unchanged except for the predicted filtering (Figures 14-15).

The mechanism is directly eliminated by the reasons shown in Section IVE. Applying filters demonstrated that the continuum emission originates from the discharge cell and not from the CCD detector and that the CCD output is a true spectrum. The artifact of the reaction of any species at the CCD is also eliminated by the observation of hydrogen continuum radiation using a channel electron multiplier (CEM) in addition to a CCD detector [2, 19].

V. Conclusions

The CfA group reproduced the published results of BlackLight Power, Inc. [1-2]. Continuum radiation was observed from pure hydrogen over the spectral region ~10 to 30 nm; whereas, no continuum was observed from helium plasmas run under essentially identical conditions. Only helium ion and background oxygen ion emission were observed; wherein, the latter was common to both plasma sources. By comparing all hydrogen results involving different electrodes, gratings, spectrometers, and numbers of CCD image superpositions, it was concluded that the same emitter was common in all cases of hydrogen continuum emission and that the spectral width varied due to variations in the spectral intensity or detection sensitivity. The hydrogen continuum radiation comprised two profiles, one with a short wavelength cutoff at about 10 nm and a second was distinguishable by a reversal of the slope of the intensity versus wavelength in the region of 22-23 nm.

Plasma physicist A. Bykanov evaluated specific known mechanisms using data from the literature and the input of further test data from BLP. Electrode metal emission was eliminated since the spectral features were the same over any given region where it was intense enough to be detected, and the intensity was shown to be proportional to concentration of hydrogen. Recombination and Bremsstrahlung radiation mechanisms were excluded because the intensities of these types of continuum spectra scale with Z as Z^2 or Z^4, respectively. Thus, we should have observed a more intense continuum spectrum in He (Z=2) than in H_2 (Z=1). Energetic electrons from an electron gun as an agent influencing the continuum band was eliminated due to the observation that changing the high voltage from -10 kV to -15 kV had no effect on the spectral profile. Band radiation for molecular electronic transitions broadened by vibrational and rotational transitions including hydrogen molecular or molecular ion emission cannot be the source due

the extraordinary energy (>100 eV) of the continuum radiation compared to the energy levels of these species. Another reason for excluding this mechanism is the broad energy width of the continuum band (~60eV) that cannot be explained by the current plasma temperature (max 15 eV, most likely <10 eV). By using spectral-region-cutoff filters and recording the spectral profile change with changing of the CCD position, the source of the continuum radiation was confirmed to be the hydrogen plasma, and the emission was deemed a true spectrum. Addition of hydrogen gas to the CCD chamber had no effect on the emission profile. These results eliminated detection artifacts as possibilities. In summary, considering the low energy of 5.2 J per pulse, the observed radiation in the photon energy range from 40 eV to 120 eV, and reference experiments with He and oxygen, no convention explanation was found to be plausible including electrode metal emission, Bremsstrahlung radiation, ion recombination, molecular or molecular ion band radiation, and instrument artifacts involving radicals and energetic ions reacting at the CCD and H_2 re-radiation at the detector.

References

1. R. L. Mills, Y. Lu, "Hydrino Continuum Transitions with Cutoffs at 22.8 nm and 10.1 nm," Int. J. Hydrogen Energy, 35 (2010), pp. 8446-8456, doi: 10.1016/j.ijhydene.2010.05.098.
2. R. L. Mills, Y. Lu, K. Akhar, "Spectroscopic Observation of Helium-Ion- and Hydrogen-Catalyzed Hydrino Transitions," Cent. Eur. J. Phys., 8 (2010), pp. 318-339, doi: 10.2478/s11534-009-0106-9.
3. R.L. Mills, K. Akhtar, G. Zhao, Z. Chang, J. He, X. Hu, G. Chu, "Commercializable Power Source Using Heterogeneous Hydrino Catalysts," Int. J. Hydrogen Energy, Vol. 35 (2010), pp. 395-419, doi: 10.1016/j.ijhydene.2009.10.038.
4. R. L. Mills, J. Lotoski, G. Zhao, K. Akhtar, Z. Chang, J. He, X. Hu, G. Wu, G. Chu, Y. Lu, "Identification of New Hydrogen States," submitted, http://www.blacklightpower.com/papers/21cm-1%20paper%20080210S.pdf.
5. D. R. Lide, CRC Handbook of Chemistry and Physics, 86th Edition, CRC Press, Taylor & Francis, Boca Raton, (2005-6), p. 4-130.
6. W.H. Bennett, Phys Rev, Vol. 45, 890 (1934).
7. Vivek Bakshi, Editor, *EUV Sources for Lithography* (SPIE Press Book), (2006), 1094 pages.
8. Ya. B. Zel'dovich, Yu. P. Raizer, *Physics of Shock Waves and High-Temperature Hydrodynamic Phenomena*, Dover Publications, (1966), 944 pages.
9. Richard H. Huddlestone, Stanley L. Leonard, et al., *Plasma Diagnostic Techniques*, Academic Press, Inc. (PCW), (1965), 627 pages.

10. A.A. Radcyg, B.M. Smirnov Handbook on atomic and molecular physics. Moscow, Atomizdat, 1980 (in Russian)
11. A. Carrington, I. R. McNab, C. A. Montgomerie, "Spectroscopy of the hydrogen molecular ion," J. Phys. B, 22, (1989), 3551–3586.
12. A. Carrington, I. R. McNab, C. A. Montgomerie, R. Kennedy, "Electronic spectrum ($2p\sigma_u$–$1s\sigma_g$) of the D_2^+ ion," Mol. Phys., 67, (1989), 711–738.
13. C. A. Leach, R. E. Moss, "Spectroscopy and quantum mechanics of the hydrogen molecular cation: A test of molecular quantum mechanics," Annu. Rev. Phys. Chem., 46, (1995), 55–82.
14. D. R. Lide, *CRC Handbook of Chemistry and Physics*, 79th Edition, CRC Press, Boca Raton, Florida, (1998-9), p. 10-175.
15. P. W. Atkins, *Physical Chemistry*, Second Edition, W. H. Freeman, San Francisco, (1982), p. 589.
16. L.C. Lee, R.W. Carlson, D.L. Judge, "The absorption cross sections of H_2 and D_2 from 180 to 780 Å," J. Quant. Spectrosc. Radiat. Transfer, Vol. 16, (1976), pp. 873-877. Comments: Absorption measurements using synchrotron radiation; spectral resolution ~0.1nm.
17. C. Back, G. R. Wight, M.J. Van der Wiel, "Oscillator strengths (10-70 eV) for absorption, ionization and dissociation in H_2, HD and D_2, obtained by an electron-ion coincidence method," J. Phys. B: Atom. Mol. Phys. 9, 315-331 (1976). Comments: Measured by dipole (e,e) spectroscopy; energies E (in eV) and differential oscillator strengths df/dE (in 10-2 eV-1) converted to wavelengths and absorption cross sections, (in 10-18 cm^2 $molecule^{-1}$) = 109.75 df/dE (in eV^{-1}).
18. J.A.R. Samson and R.B. Cairns, "Total absorption cross sections of H_2, N_2, and O_2 in the region 550-220 Å," J. Opt. Soc. Am., Vol. 45, (1965), p.1035.
19. A. F. H. van Gessel, Masters Thesis: *EUV spectroscopy of hydrogen plasmas*, April (2009), Eindhoven University of Technology, Department of Applied Physics, Group of Elementary Processes in Gas Discharges, EPG 09-02, pp. 61-70.

Figure 1. Experimental setup for the high-voltage pulsed discharge cell. The source emits its light spectra through an entrance aperture passing through a slit, with the spectra dispersed off a grazing-incidence grating onto a CCD detection system.

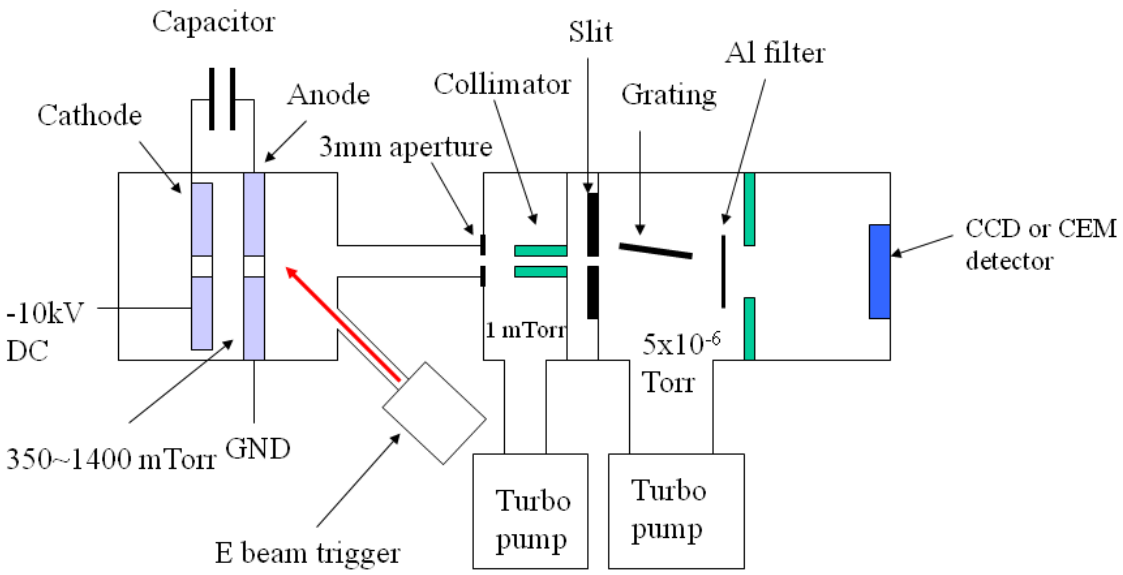

Figure 2. Photograph of the BLP high-voltage pulsed discharge light source.

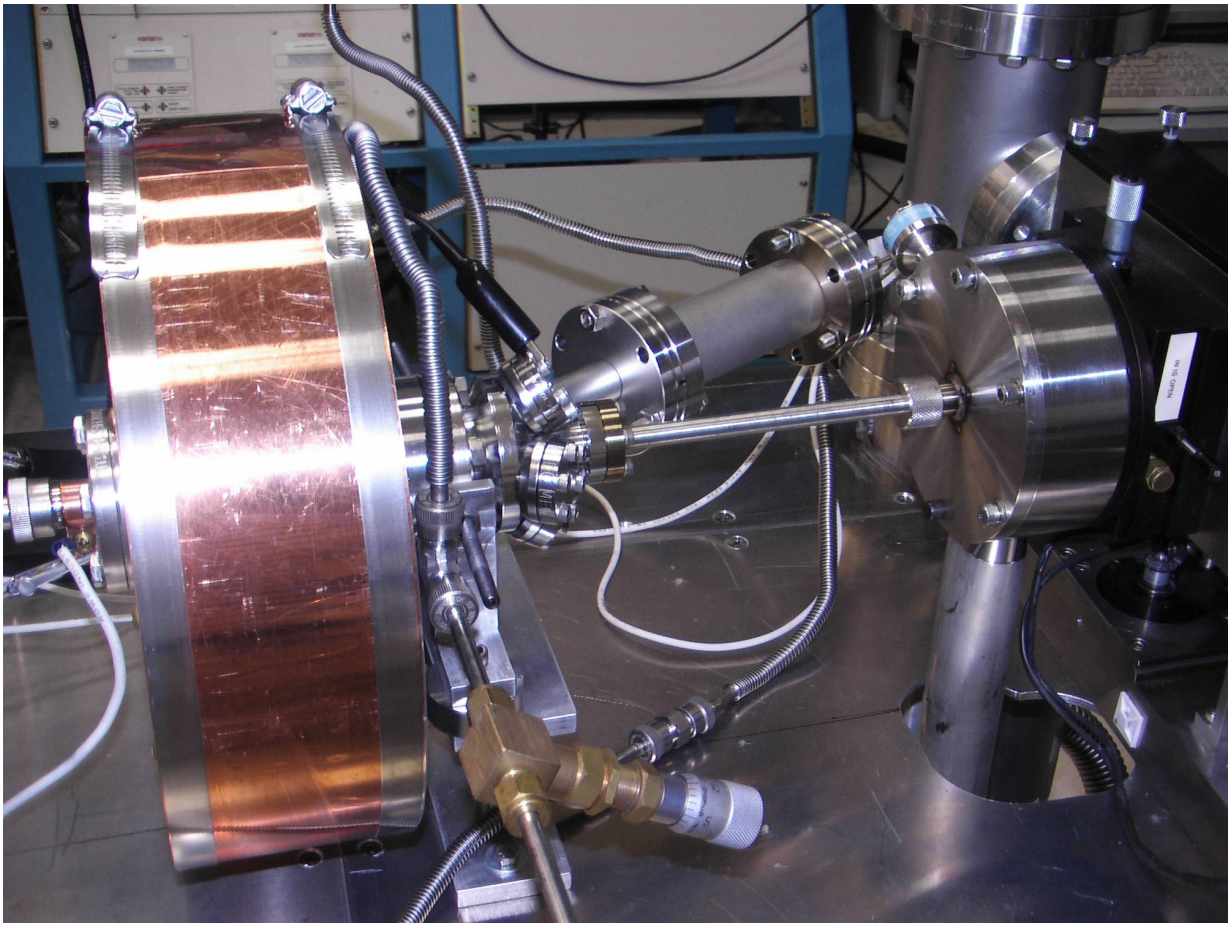

Figures 3A-D. Emission spectra (12.5-33 nm) of electron-beam-initiated, high-voltage pulsed discharges in helium. Only known helium and oxygen ion lines were observed in the absence of a continuum. (A) Plasma maintained with Ta electrodes, and emission recorded using the BLP EUV grazing incidence spectrometer with the BLP 1200 lines/mm grating and 500 superpositions. (B) Plasma maintained with Ta electrodes, and emission recorded using the CfA EUV grazing incidence spectrometer with the CfA 1200 lines/mm grating and 500 superpositions. (C) Plasma maintained with W electrodes, and emission recorded using the BLP EUV grazing incidence spectrometer with the BLP 1200 lines/mm grating and 500 superpositions. (D) Plasma maintained with W electrodes, and emission recorded using the CfA EUV grazing incidence spectrometer with the CfA 1200 lines/mm grating and 500 superpositions.

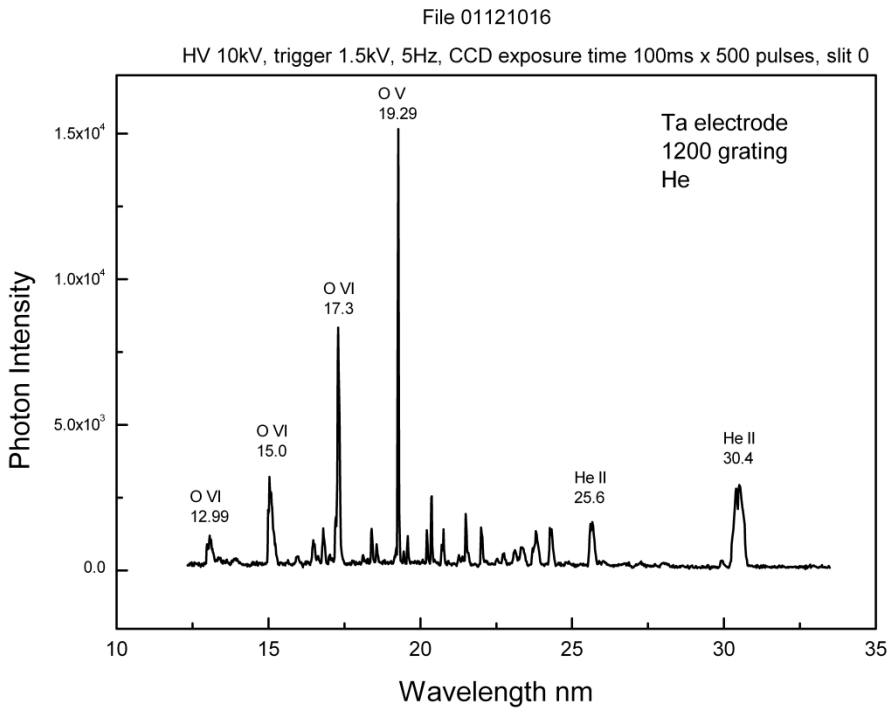

(A)

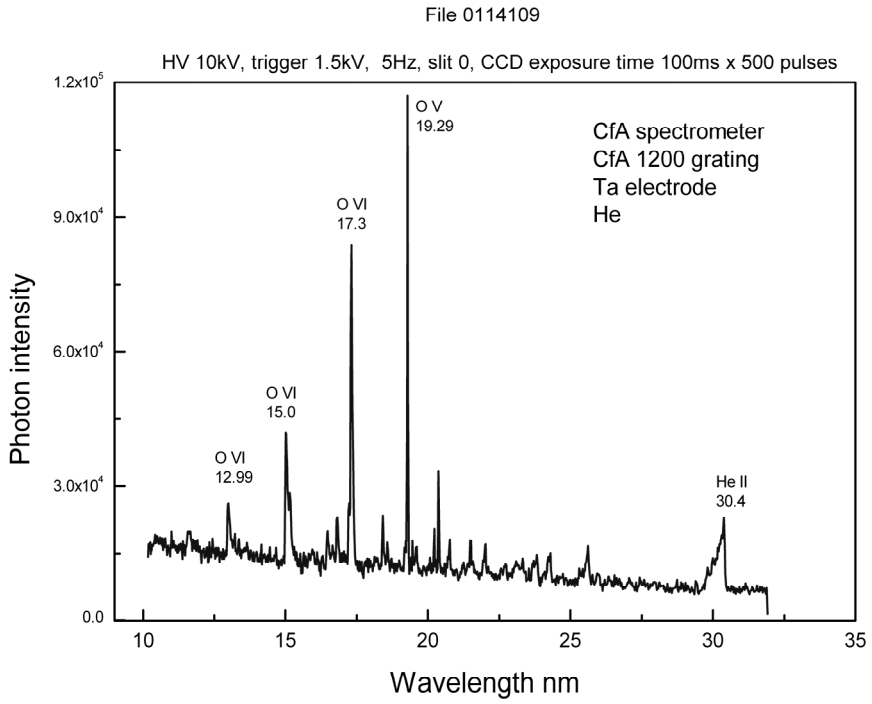
File 0114109
HV 10kV, trigger 1.5kV, 5Hz, slit 0, CCD exposure time 100ms x 500 pulses
CfA spectrometer
CfA 1200 grating
Ta electrode
He
O V
19.29
O VI
17.3
O VI
15.0
O VI
12.99
He II
30.4
Photon intensity
Wavelength nm

(B)

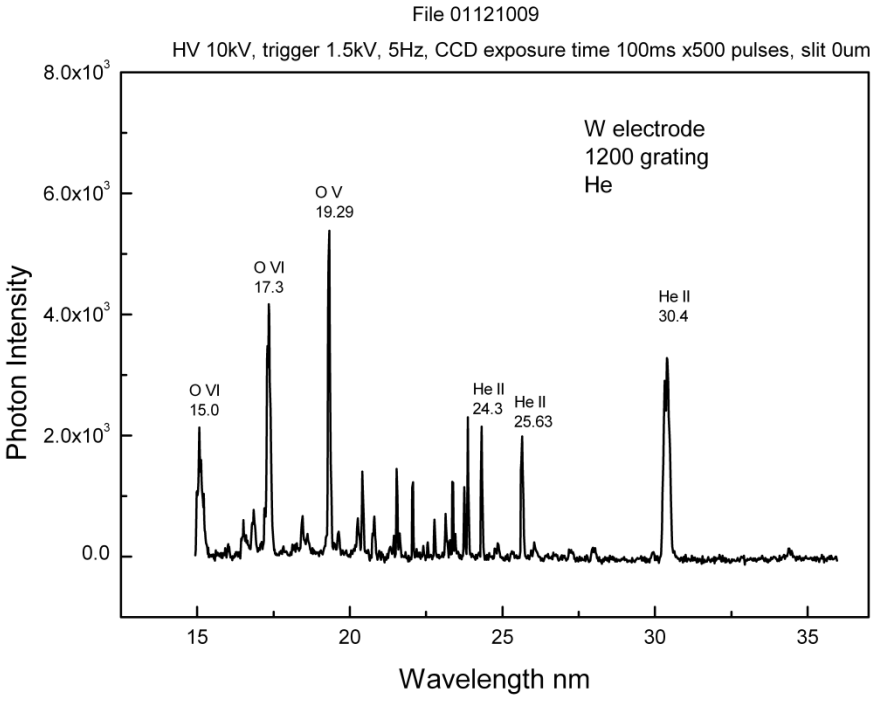
File 01121009
HV 10kV, trigger 1.5kV, 5Hz, CCD exposure time 100ms x500 pulses, slit 0um
W electrode
1200 grating
He
O V
19.29
O VI
17.3
O VI
15.0
He II
30.4
He II
24.3
He II
25.63
Photon Intensity
Wavelength nm

(C)

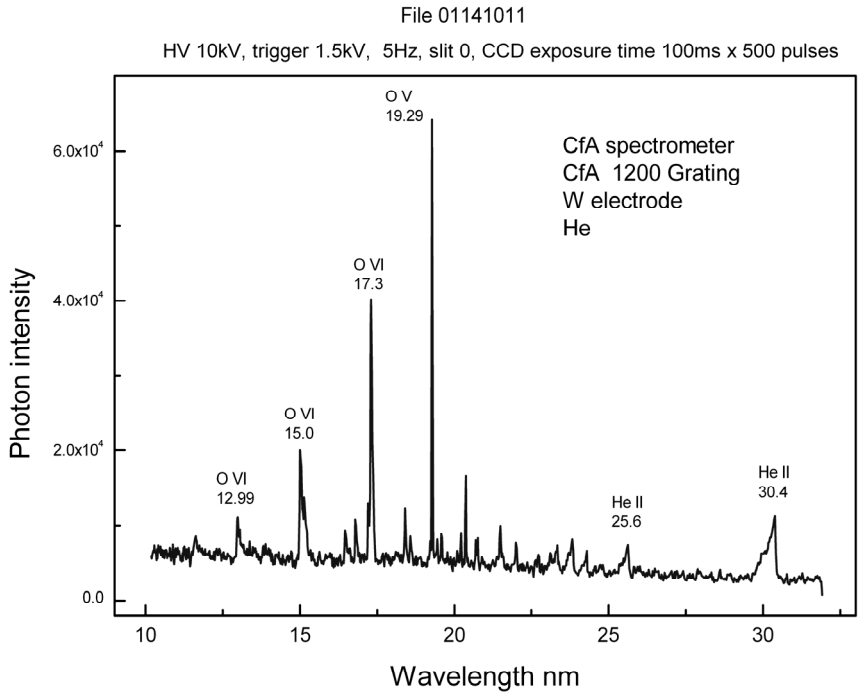
File 01141011
HV 10kV, trigger 1.5kV, 5Hz, slit 0, CCD exposure time 100ms x 500 pulses
CfA spectrometer
CfA 1200 Grating
W electrode
He
O V
19.29
O VI
17.3
O VI
15.0
O VI
12.99
He II
25.6
He II
30.4
Photon intensity
6.0x10^4
4.0x10^4
2.0x10^4
0.0
10
15
20
25
30
Wavelength nm

(D)

Figures 4A-J. Emission spectra (2.5-45 nm) of electron-beam-initiated, high-voltage pulsed gas discharges in helium or hydrogen. Only known helium and oxygen ion lines were observed with helium. Continuum radiation was observed for hydrogen only independent of the electrode, grating, spectrometer, or number of CCD image superpositions. (A) Helium and hydrogen plasmas maintained with Mo electrodes and emission recorded using the BLP EUV grazing incidence spectrometer with the BLP 1200 lines/mm grating and 500 superpositions. (B) Helium and hydrogen plasmas maintained with Mo electrodes and emission recorded using the CfA EUV grazing incidence spectrometer with the CfA 1200 lines/mm grating and 500 superpositions. (C) Helium and hydrogen plasmas maintained with Mo electrodes and emission recorded using the CfA EUV grazing incidence spectrometer with the BLP 600 lines/mm grating and 1000 superpositions. (D) Hydrogen plasma maintained with Ta electrodes and emission recorded using the BLP EUV grazing incidence spectrometer with the BLP 1200 lines/mm grating and 500 superpositions. (E) Helium and hydrogen plasmas maintained with Ta electrodes and emission recorded using the CfA EUV grazing incidence spectrometer with the BLP 600 lines/mm grating and 1000 superpositions. (F) Hydrogen plasma maintained with W electrodes and emission recorded using the BLP EUV grazing incidence spectrometer with the BLP 1200 lines/mm grating and 500 superpositions. (G) Hydrogen plasma maintained with W electrodes and emission recorded using the CfA EUV grazing incidence spectrometer with the CfA 1200 lines/mm grating and 500 superpositions. (H) Hydrogen plasma maintained with W electrodes and emission recorded using the CfA EUV grazing incidence spectrometer with the CfA 1200 lines/mm grating and 5000 superpositions. (I) Helium and hydrogen plasmas maintained with W electrodes and emission recorded using the CfA EUV grazing incidence spectrometer with the CfA 1200 lines/mm grating and 1000 superpositions. (J) Helium and hydrogen plasmas maintained with W electrodes and emission recorded using the CfA EUV grazing incidence spectrometer with the BLP 600 lines/mm grating and 1000 superpositions.

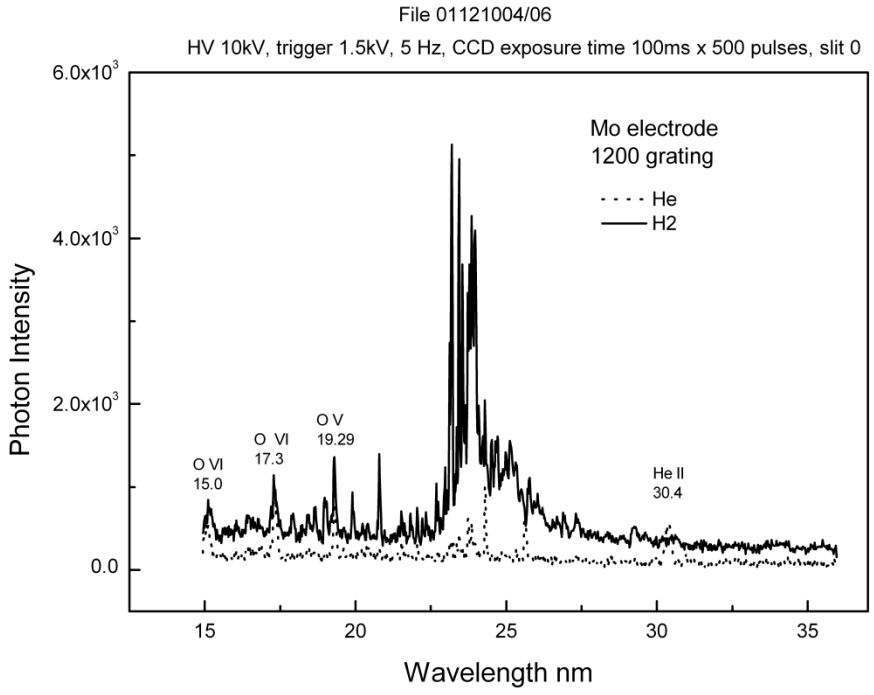
File 01121004/06
HV 10kV, trigger 1.5kV, 5 Hz, CCD exposure time 100ms x 500 pulses, slit 0
Mo electrode
1200 grating
He
H2
Photon Intensity
Wavelength nm
O VI 15.0
O VI 17.3
O V 19.29
He II 30.4

(A)

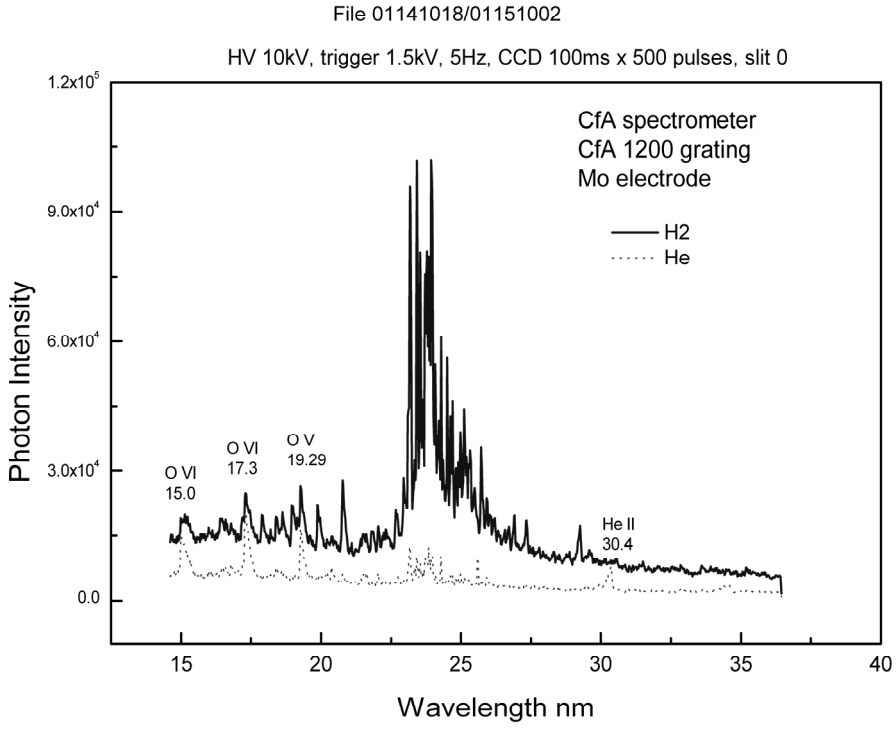
File 01141018/01151002
HV 10kV, trigger 1.5kV, 5Hz, CCD 100ms x 500 pulses, slit 0
CfA spectrometer
CfA 1200 grating
Mo electrode
H2
He
Photon Intensity
Wavelength nm
O VI 15.0
O VI 17.3
O V 19.29
He II 30.4

(B)

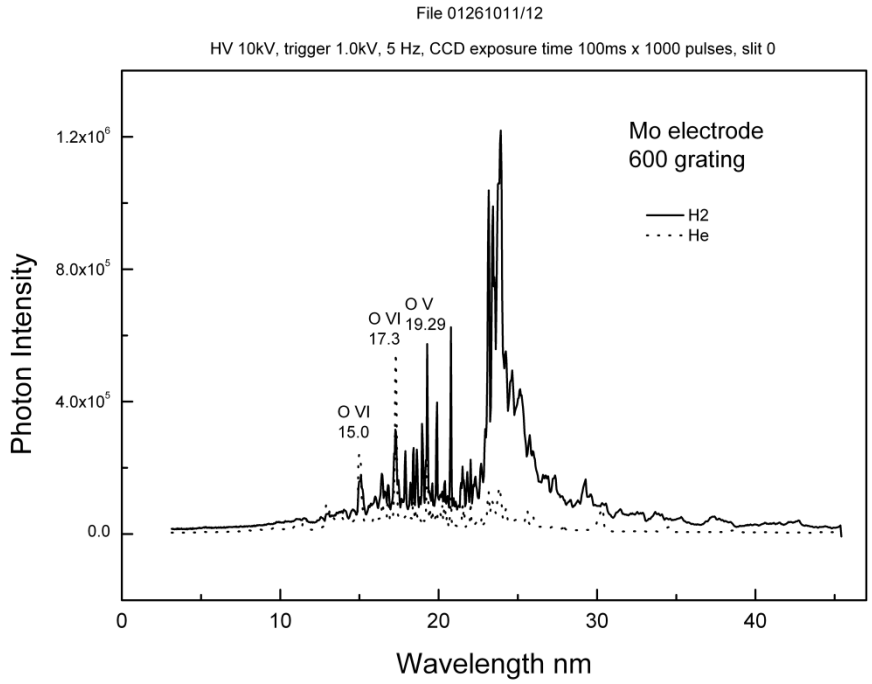
File 01261011/12
HV 10kV, trigger 1.0kV, 5 Hz, CCD exposure time 100ms x 1000 pulses, slit 0
Mo electrode
600 grating
H2
He
O VI
15.0
O VI
17.3
O V
19.29
Photon Intensity
Wavelength nm
1.2x10^6
8.0x10^5
4.0x10^5
0.0
0
10
20
30
40

(C)

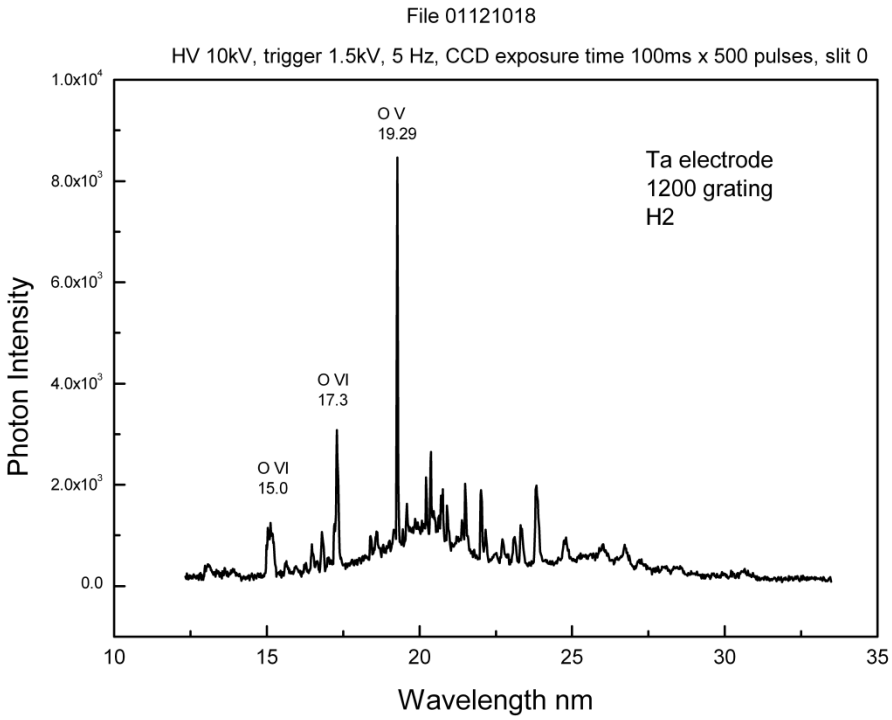
File 01121018
HV 10kV, trigger 1.5kV, 5 Hz, CCD exposure time 100ms x 500 pulses, slit 0
Ta electrode
1200 grating
H2
O V
19.29
O VI
17.3
O VI
15.0
Photon Intensity
Wavelength nm
1.0x10^4
8.0x10^3
6.0x10^3
4.0x10^3
2.0x10^3
0.0
10
15
20
25
30
35

(D)

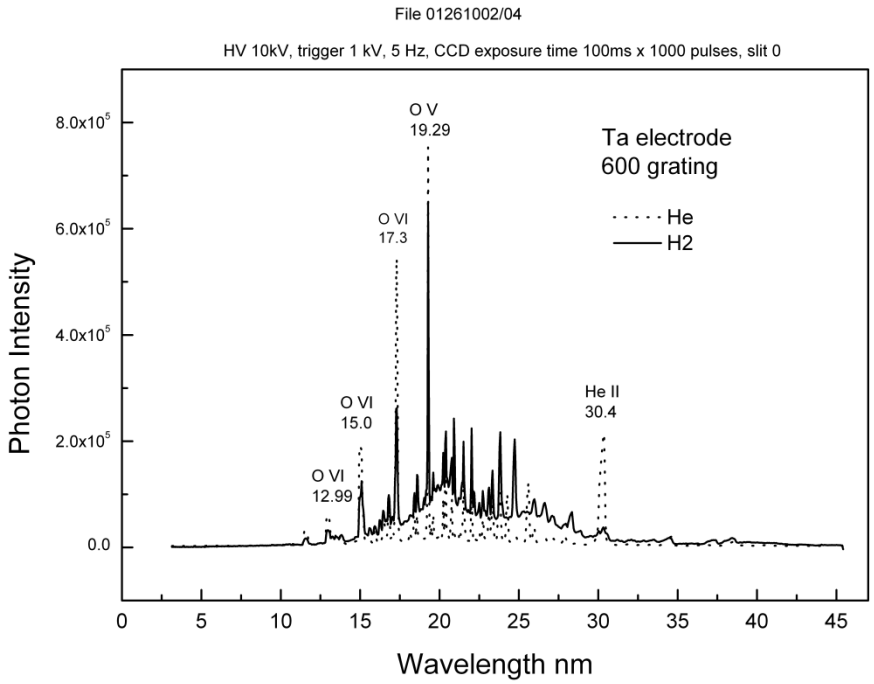
File 01261002/04
HV 10kV, trigger 1 kV, 5 Hz, CCD exposure time 100ms x 1000 pulses, slit 0
Photon Intensity
Wavelength nm
O V
19.29
O VI
17.3
O VI
15.0
O VI
12.99
He II
30.4
Ta electrode
600 grating
He
H2

(E)

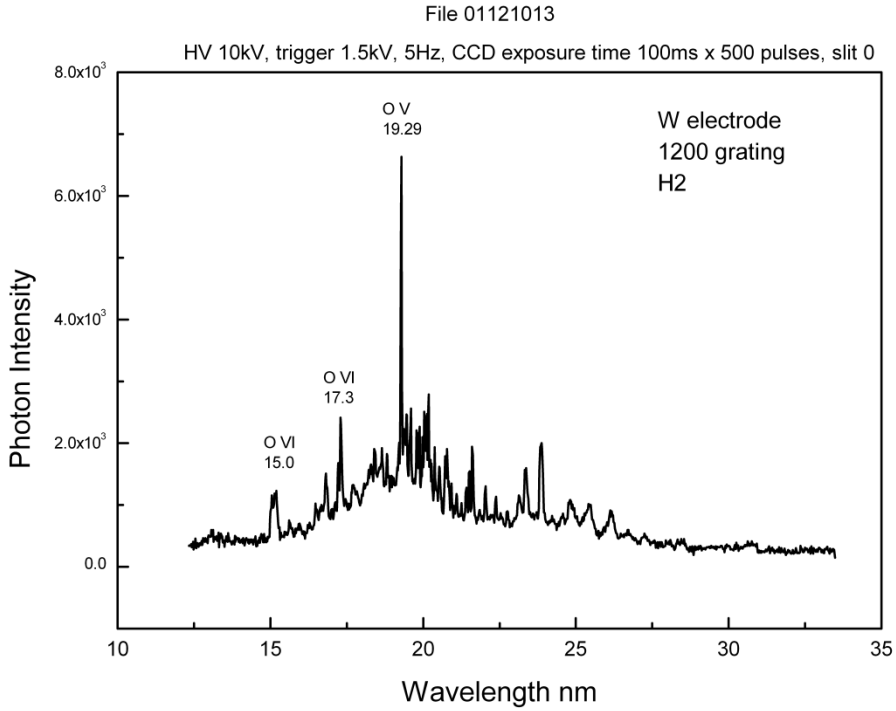
File 01121013
HV 10kV, trigger 1.5kV, 5Hz, CCD exposure time 100ms x 500 pulses, slit 0
Photon Intensity
Wavelength nm
O V
19.29
O VI
17.3
O VI
15.0
W electrode
1200 grating
H2

(F)

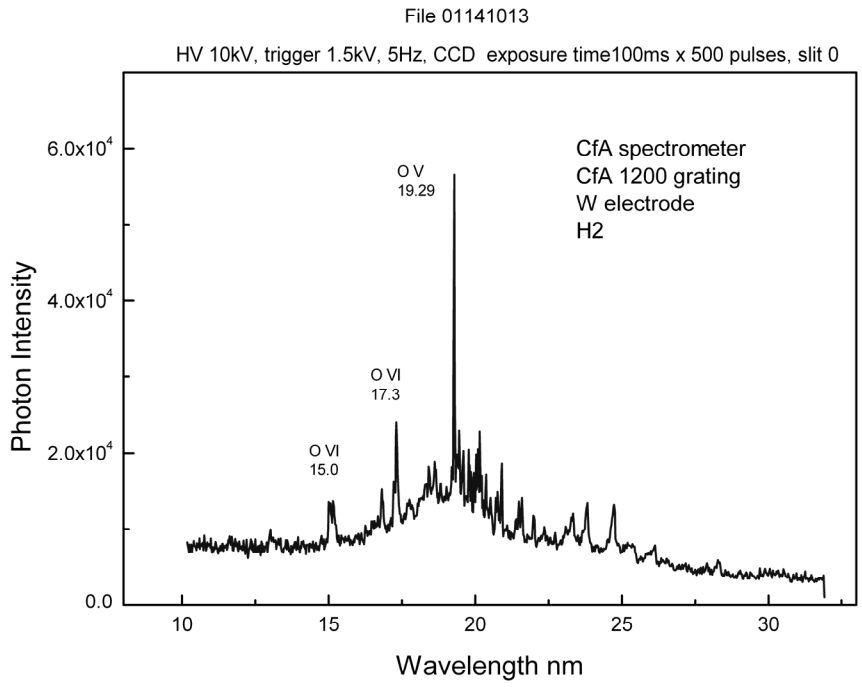
File 01141013
HV 10kV, trigger 1.5kV, 5Hz, CCD exposure time100ms x 500 pulses, slit 0
CfA spectrometer
CfA 1200 grating
W electrode
H2
O V
19.29
O VI
17.3
O VI
15.0
Photon Intensity
6.0x10^4
4.0x10^4
2.0x10^4
0.0
10
15
20
25
30
Wavelength nm

(G)

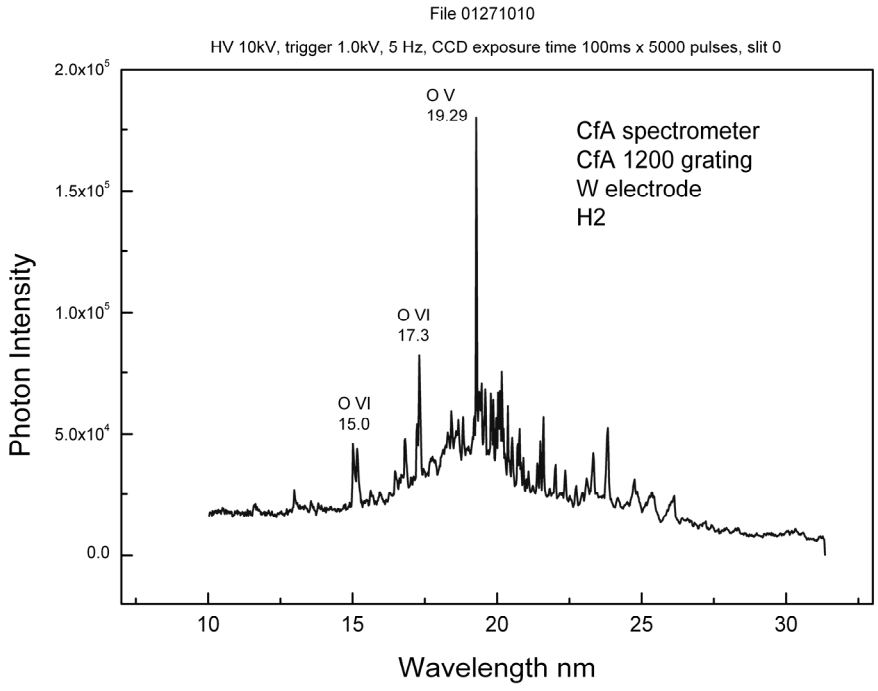
File 01271010
HV 10kV, trigger 1.0kV, 5 Hz, CCD exposure time 100ms x 5000 pulses, slit 0
CfA spectrometer
CfA 1200 grating
W electrode
H2
O V
19.29
O VI
17.3
O VI
15.0
Photon Intensity
2.0x10^5
1.5x10^5
1.0x10^5
5.0x10^4
0.0
10
15
20
25
30
Wavelength nm

(H)

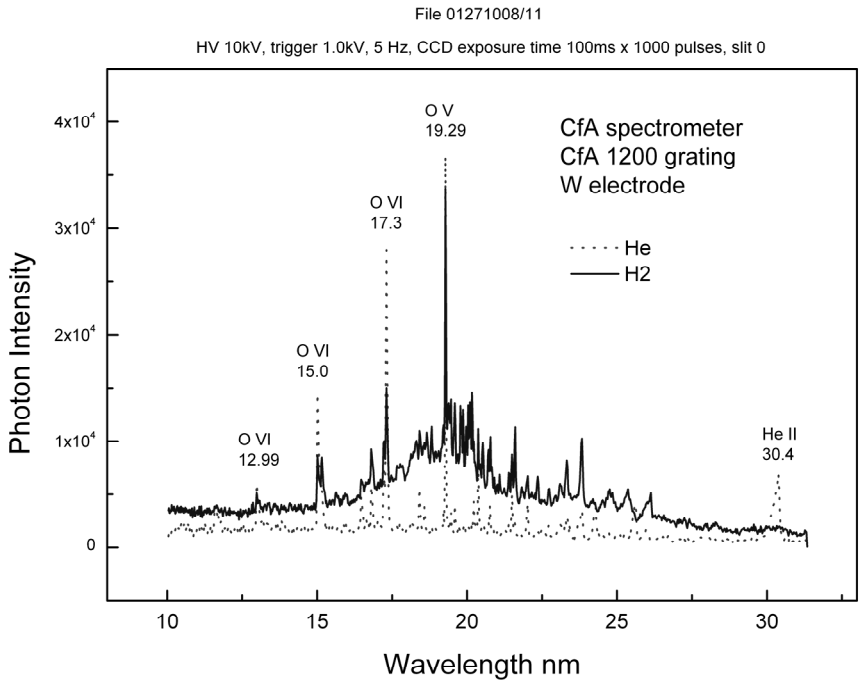
File 01271008/11
HV 10kV, trigger 1.0kV, 5 Hz, CCD exposure time 100ms x 1000 pulses, slit 0
CfA spectrometer
CfA 1200 grating
W electrode
He
H2
O V
19.29
O VI
17.3
O VI
15.0
O VI
12.99
He II
30.4
Photon Intensity
Wavelength nm

(I)

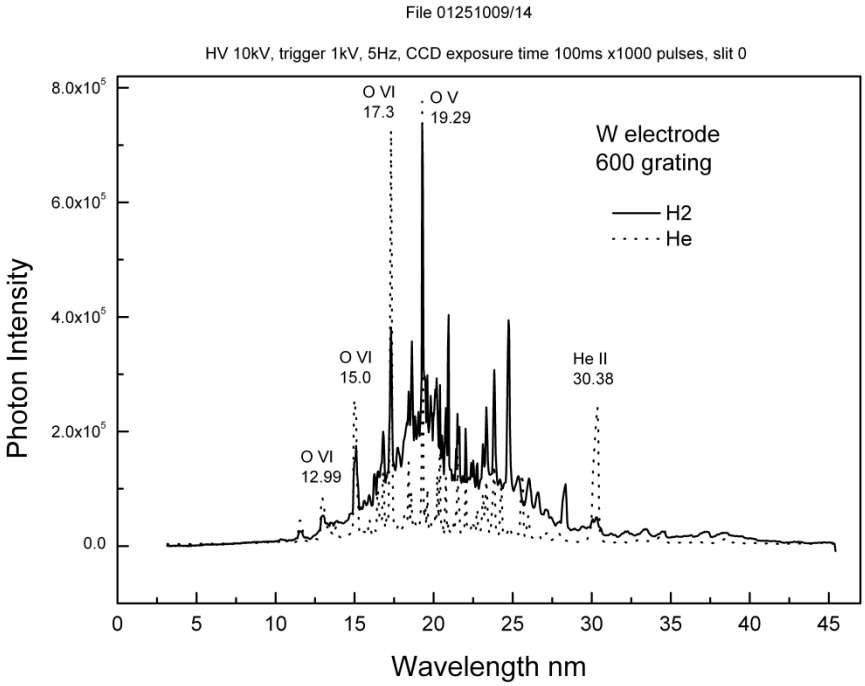
File 01251009/14
HV 10kV, trigger 1kV, 5Hz, CCD exposure time 100ms x1000 pulses, slit 0
W electrode
600 grating
H2
He
O VI
17.3
O V
19.29
O VI
15.0
O VI
12.99
He II
30.38
Photon Intensity
Wavelength nm

(J)

Figures 5A-B. Emission spectra (5-45 nm) of electron-beam-initiated, high-voltage pulsed discharges in oxygen and oxygen-hydrogen mixture. (A) Pure oxygen plasma (90 mTorr) maintained with Ta electrodes, and emission recorded using the BLP EUV grazing incidence spectrometer with the BLP 600 lines/mm grating and 1000 superpositions. Only known oxygen ion lines were observed in the absence of a continuum. (B) Oxygen (45mTorr)-hydrogen (255 mTorr) plasma maintained with Ta electrodes, and emission recorded using the BLP EUV grazing incidence spectrometer with the BLP 600 lines/mm grating and 1000 superpositions. A weak continuum was observed.

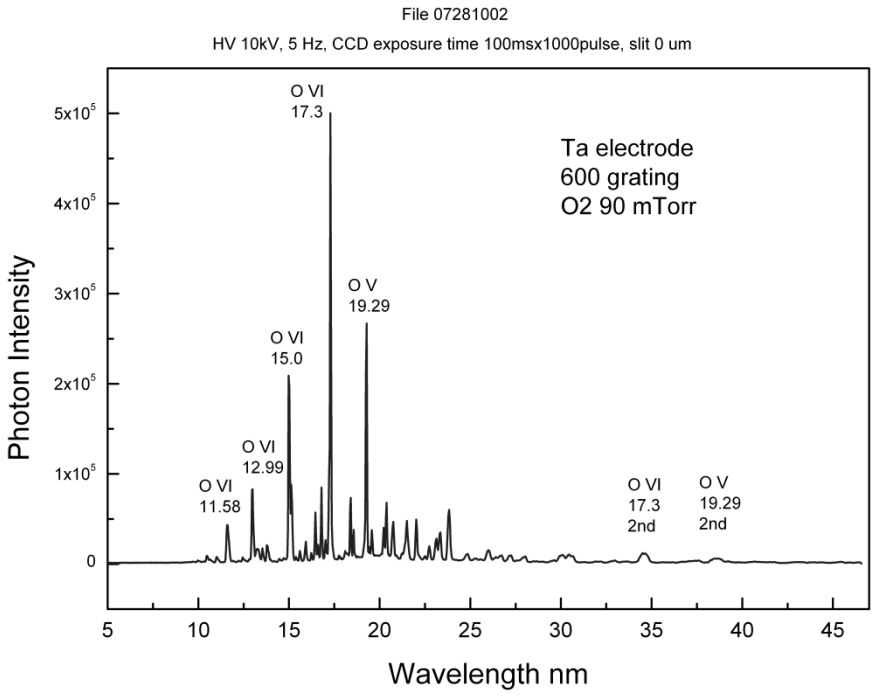

(A)

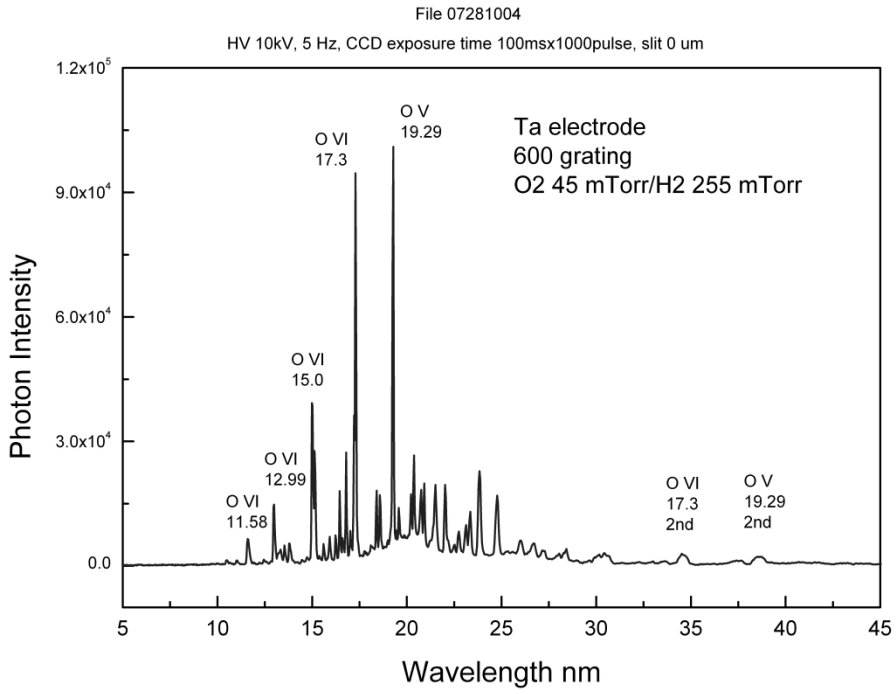
File 07281004
HV 10kV, 5 Hz, CCD exposure time 100msx1000pulse, slit 0 um
Ta electrode
600 grating
O2 45 mTorr/H2 255 mTorr
O VI 11.58
O VI 12.99
O VI 15.0
O VI 17.3
O V 19.29
O VI 17.3 2nd
O V 19.29 2nd
Photon Intensity
Wavelength nm
1.2x10^5
9.0x10^4
6.0x10^4
3.0x10^4
0.0
5
10
15
20
25
30
35
40
45

(B)

Figure 6. Emission spectra (10-35 nm) of electron-beam-initiated, high-voltage pulsed discharges in helium-hydrogen mixtures with W electrodes recorded by the BLP EUV grazing incidence spectrometer using the BLP 600 lines/mm grating and 1000 superpositions showing that the continuum radiation increased in intensity with increasing hydrogen pressure.

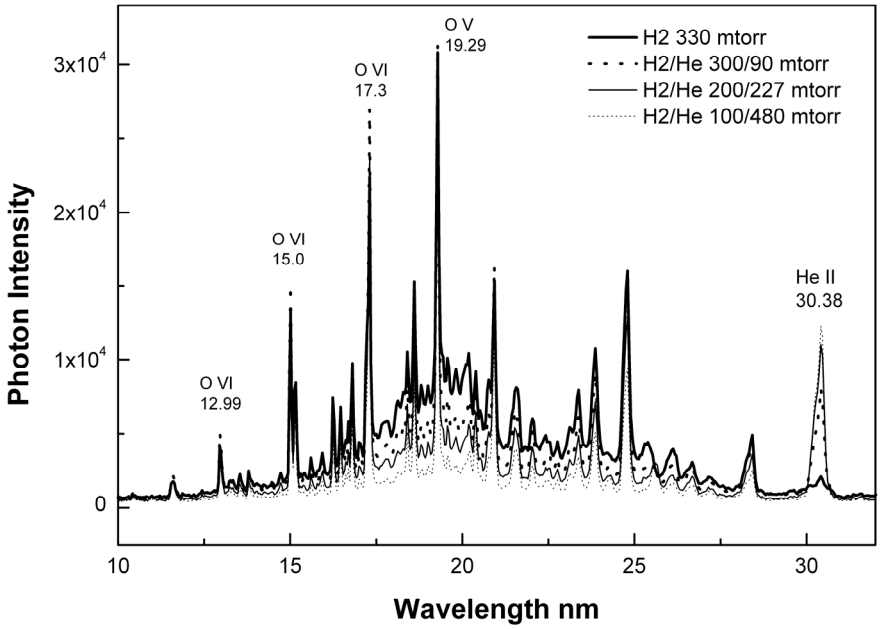

Figure 7. Emission spectrum (8-30 nm) of an electron-beam-initiated, high-voltage pulsed discharge in hydrogen using Ta electrodes recorded with the BLP EUV grazing incidence spectrometer with the BLP 600 lines/mm grating and 5000 superpositions having the CCD focused at 10 nm to enhance the sensitivity at the short-wavelength cutoff region. The cutoff of the continuum radiation is at about 10 nm.

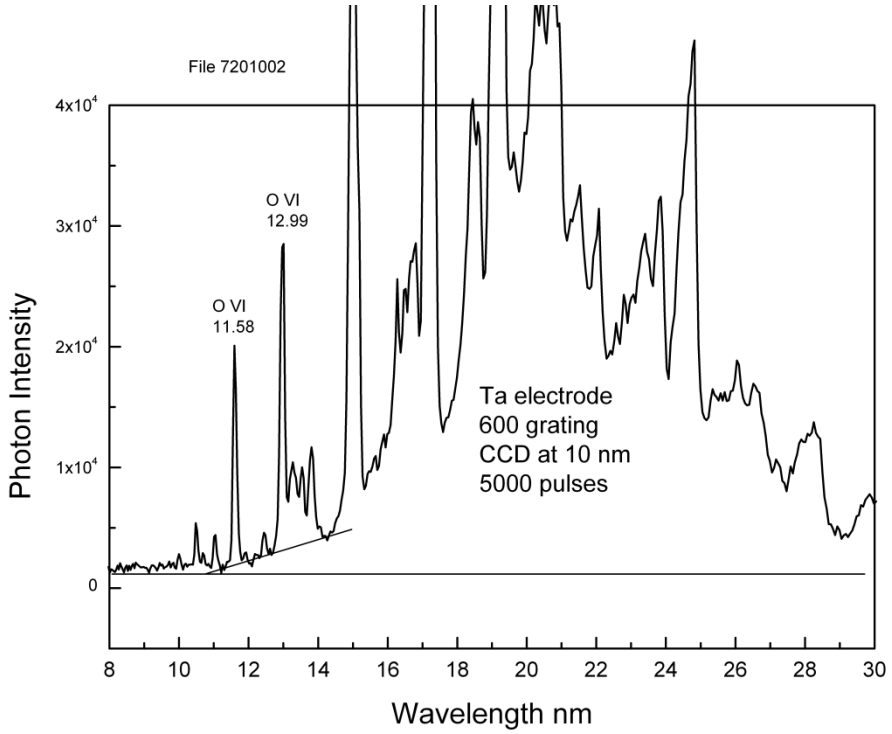

Figure 8. Cross-section of the dense plasma focus (DPF) discharge chamber designed and developed at Cymer in San Diego.

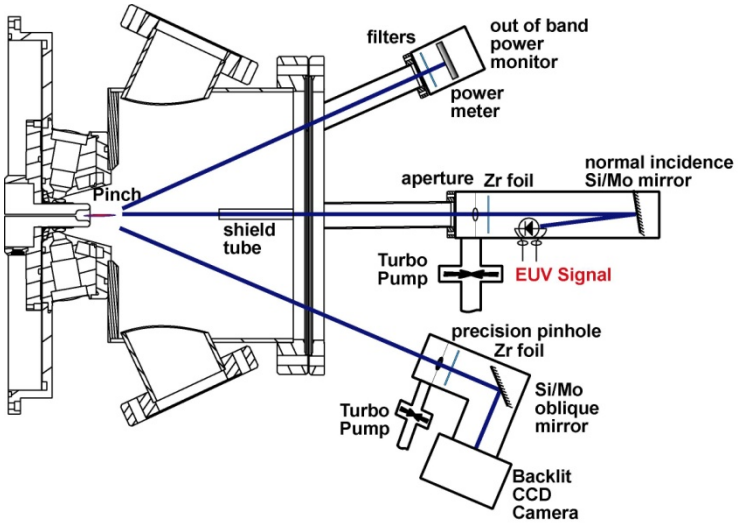

Figure 9. Diagram of the energies and corresponding terms of H_2 and the single term of H_2^+.

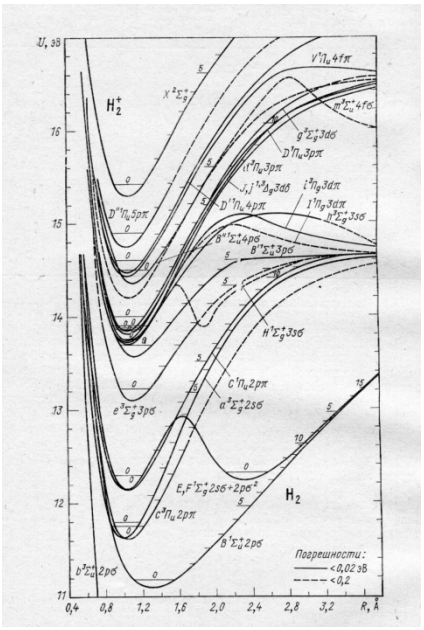

Figure 10. Absorption cross-section for H_2 and He. LBL database and experimental data as indicated.

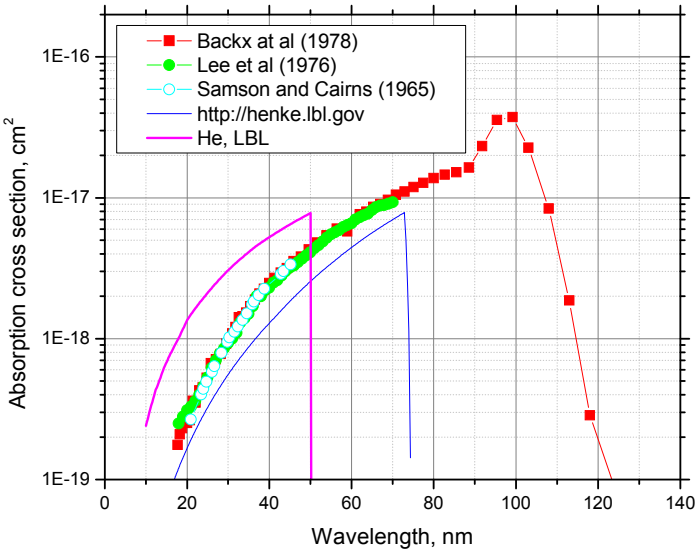

Figures 11A-C. Emission spectra (2.5-45 nm) of electron-beam-initiated, high-voltage pulsed discharges in hydrogen and helium with Ta electrodes recorded by the BLP EUV grazing incidence spectrometer using the BLP 600 lines/mm grating at background pressure and with relatively high hydrogen pressures added to the CCD chamber showing that the hydrogen addition had no effect on the spectral profile of the continuum radiation from hydrogen or the ion radiation from both plasmas. The continuum radiation source is the plasma, and it is not due to H_2 re-radiation at the detector corresponding to an artifact. (A) Helium plasma with and without hydrogen addition to the CCD chamber at a pressure of 2.2 mTorr. (B) Hydrogen plasma with and without hydrogen addition to the CCD chamber at a pressure of 2.2 mTorr. (C) Hydrogen plasma with and without hydrogen addition to the CCD chamber at a pressure of 5.1 mTorr.

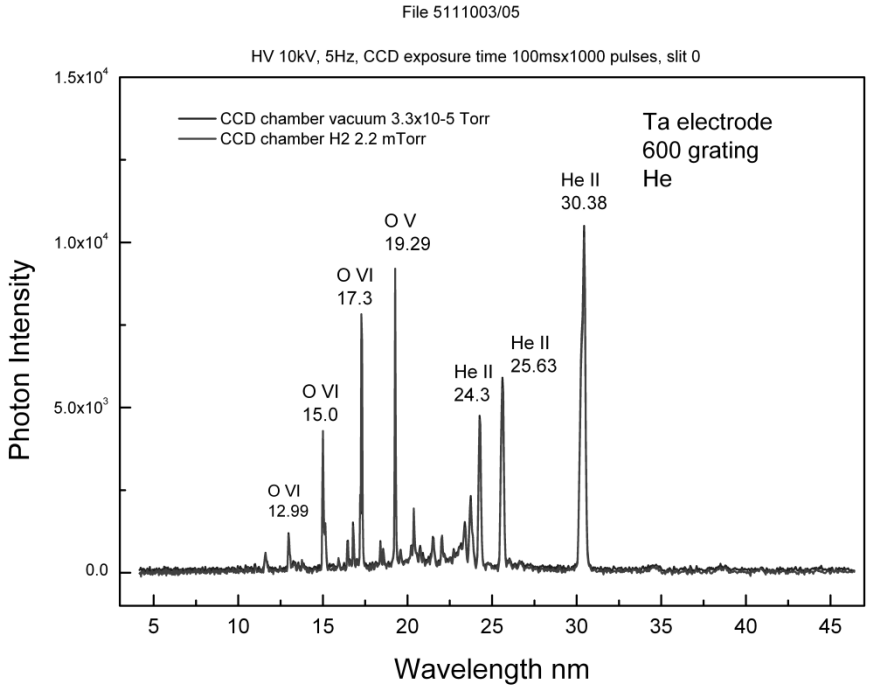

(A)

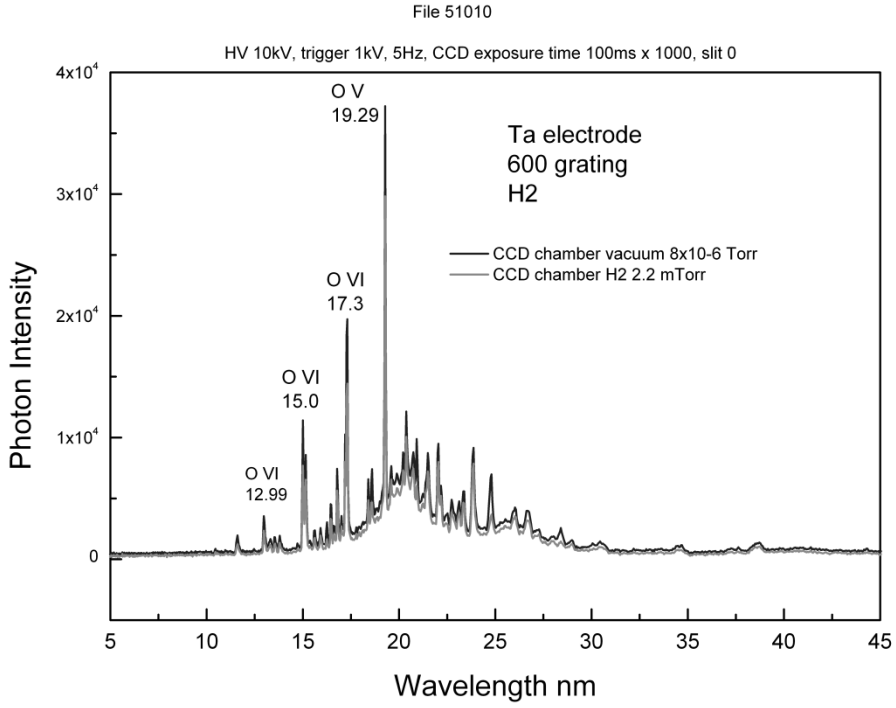
File 51010
HV 10kV, trigger 1kV, 5Hz, CCD exposure time 100ms x 1000, slit 0
Photon Intensity
Wavelength nm
O V
19.29
O VI
17.3
O VI
15.0
O VI
12.99
Ta electrode
600 grating
H2
CCD chamber vacuum 8x10-6 Torr
CCD chamber H2 2.2 mTorr

(B)

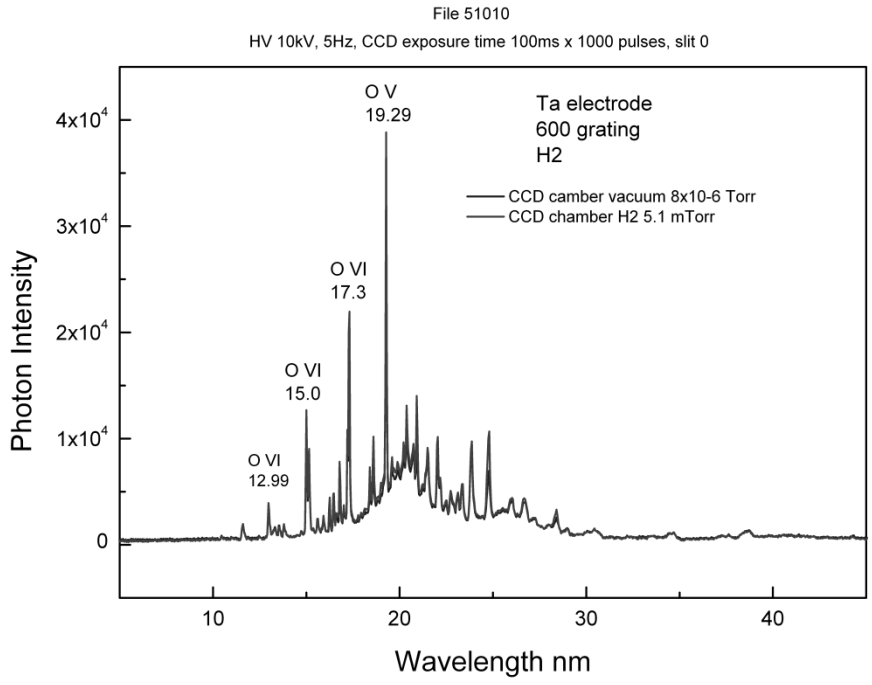
File 51010
HV 10kV, 5Hz, CCD exposure time 100ms x 1000 pulses, slit 0
Photon Intensity
Wavelength nm
O V
19.29
O VI
17.3
O VI
15.0
O VI
12.99
Ta electrode
600 grating
H2
CCD camber vacuum 8x10-6 Torr
CCD chamber H2 5.1 mTorr

(C)

Figure 12. Transmission curve of the Al filter (150 nm thickness) having a cutoff to short wavelengths at ~17 nm.

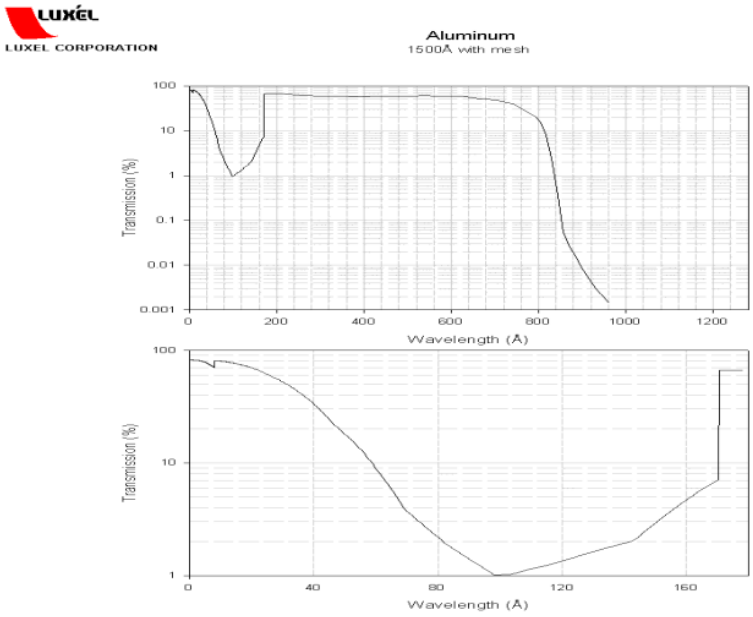

Figure 13. Transmission curve of the polyimide filter (110 nm thickness) having a cutoff to the long-wavelengths side of the continuum spectral region.

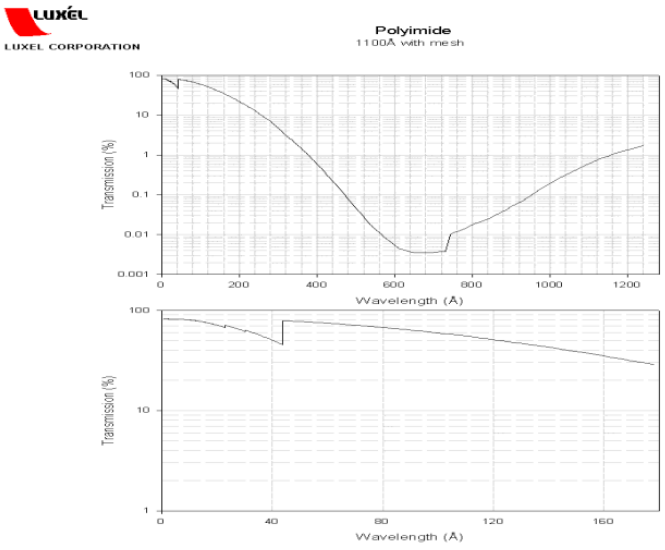

Figures 14A-C. Emission spectra (2.5-45 nm) of electron-beam-initiated, high-voltage pulsed discharges in hydrogen and helium with Ta or W electrodes recorded by the BLP EUV grazing incidence spectrometer using the BLP 600 lines/mm grating and the Al filter (150 nm thickness) showing that the continuum radiation from hydrogen and ion radiation from both plasmas had a cut-off at the 17 nm corresponding to the edge of the Al filter shown in Figure 12. The continuum radiation source is the plasma and not remote from it corresponding to an artifact. (A) Helium plasma with and without the Al filter. (B) Hydrogen plasma with the Al filter. (C) Hydrogen plasma with and without the Al filter.

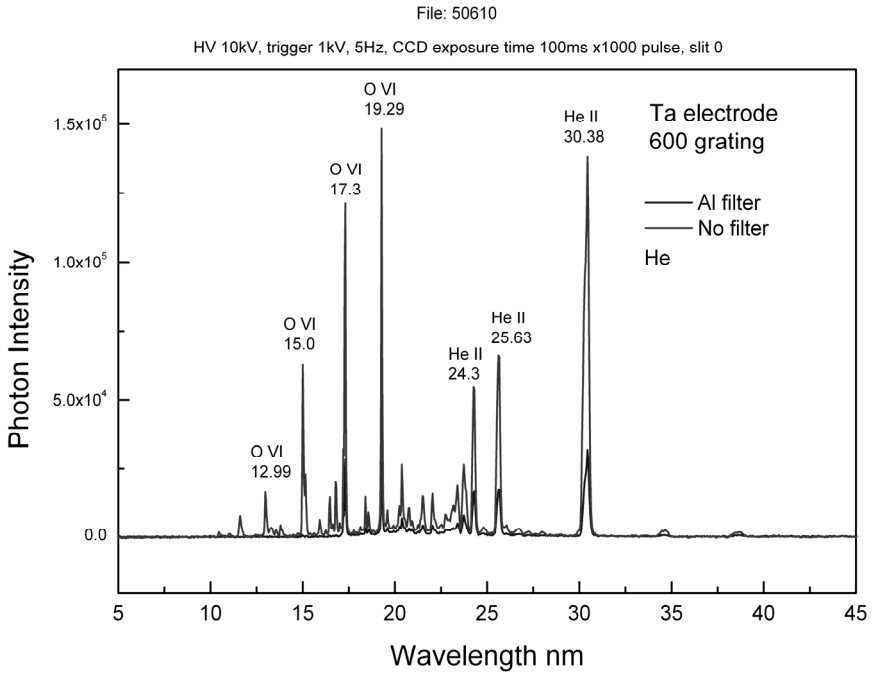

(A)

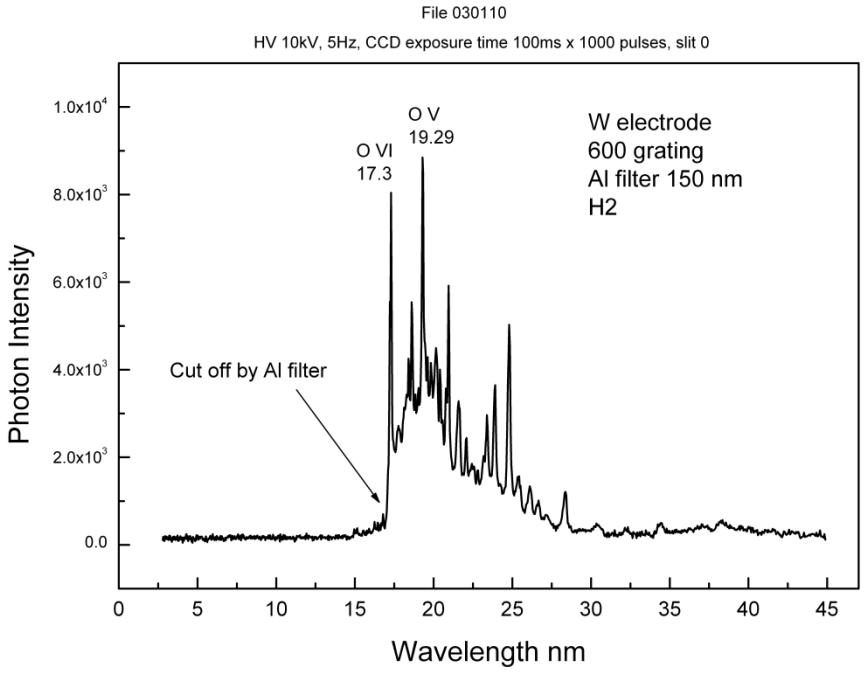
File 030110
HV 10kV, 5Hz, CCD exposure time 100ms x 1000 pulses, slit 0
Photon Intensity
Wavelength nm
W electrode
600 grating
Al filter 150 nm
H2
O VI
17.3
O V
19.29
Cut off by Al filter

(B)

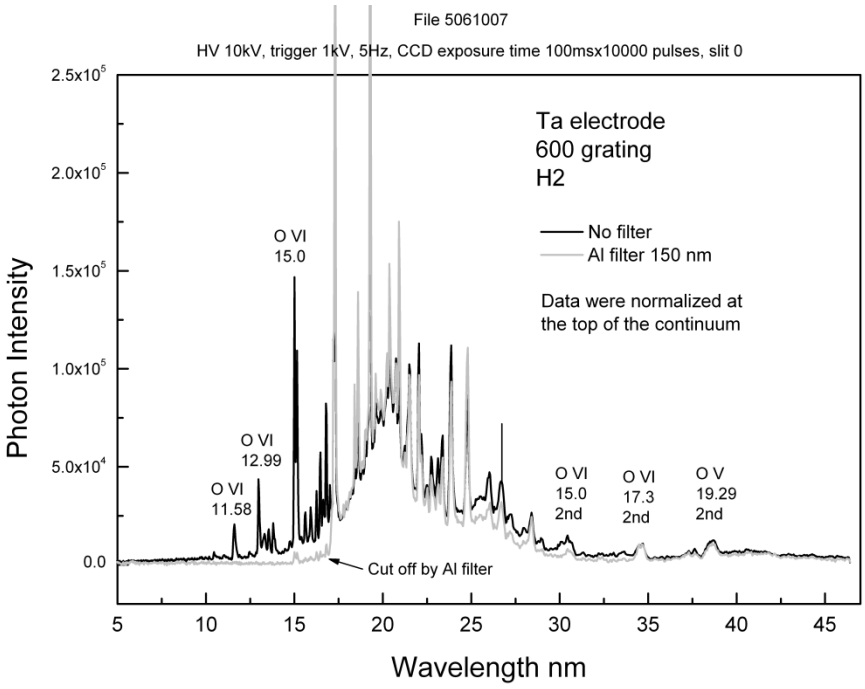
File 5061007
HV 10kV, trigger 1kV, 5Hz, CCD exposure time 100msx10000 pulses, slit 0
Photon Intensity
Wavelength nm
Ta electrode
600 grating
H2
No filter
Al filter 150 nm
Data were normalized at
the top of the continuum
O VI
15.0
O VI
12.99
O VI
11.58
O VI
15.0
2nd
O VI
17.3
2nd
O V
19.29
2nd
Cut off by Al filter

(C)

GEN3 PARTNERS

Figure 15A-B. Emission spectra (2.5-45 nm) of electron-beam-initiated, high-voltage pulsed discharges in hydrogen and helium with Ta electrodes recorded by the BLP EUV grazing incidence spectrometer using the BLP 600 lines/mm grating and the polyimide filter (110 nm thickness) showing that the continuum radiation from hydrogen and ion radiation from both plasmas had a cut-off on the long wavelength side corresponding to the transmission curve of the polyimide filter shown in Figure 13. The continuum radiation source is the plasma and not remote from it corresponding to an artifact. (A) Helium plasma with and without the polyimide filter. (B) Hydrogen plasma with and without the polyimide filter.

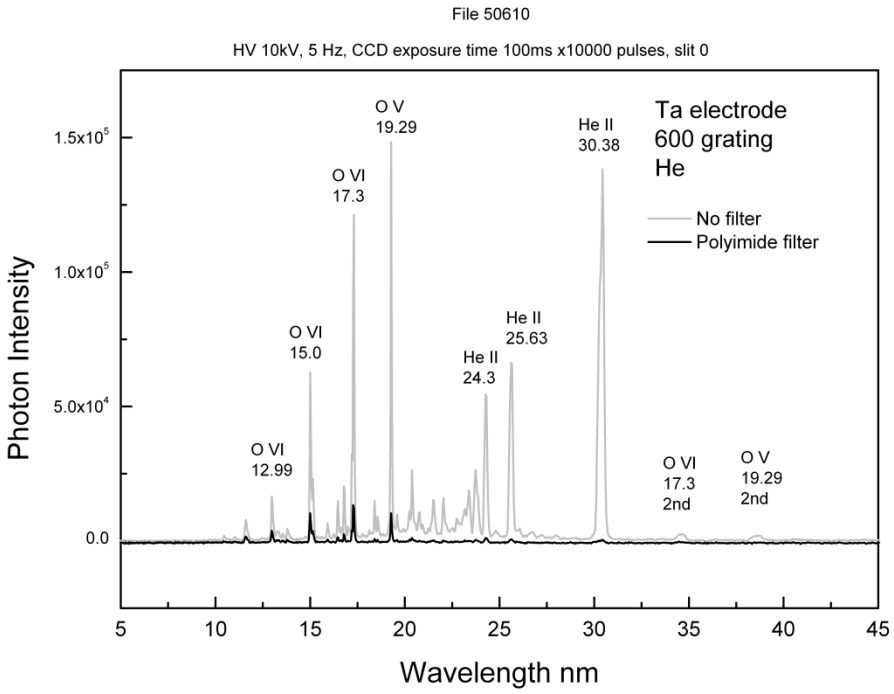

(A)

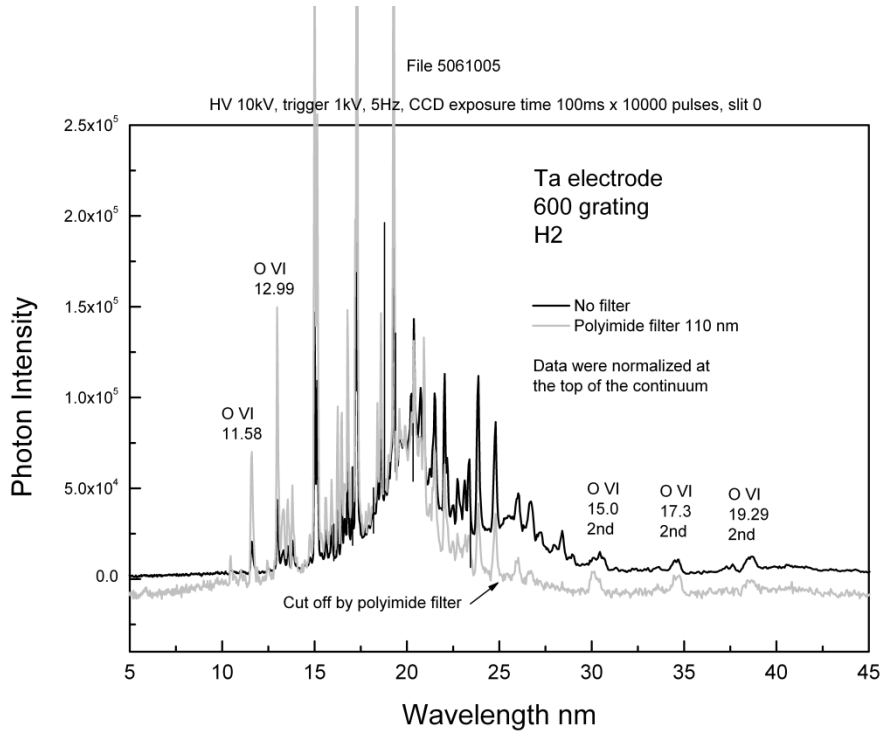
File 5061005
HV 10kV, trigger 1kV, 5Hz, CCD exposure time 100ms x 10000 pulses, slit 0
Ta electrode
600 grating
H2
No filter
Polyimide filter 110 nm
Data were normalized at
the top of the continuum
O VI
12.99
O VI
11.58
O VI
15.0
2nd
O VI
17.3
2nd
O VI
19.29
2nd
Cut off by polyimide filter
Photon Intensity
Wavelength nm
2.5x10^5
2.0x10^5
1.5x10^5
1.0x10^5
5.0x10^4
0.0
5
10
15
20
25
30
35
40
45

(B)